The anterior Hox gene *ceh-13* and *elt-1/GATA* activate the posterior Hox genes *nob-1* and *php-3* to specify posterior lineages in the *C. elegans* embryo

John Isaac Murray[2], Elicia Preston[2], Jeremy P. Crawford[1], Jonathan D. Rumley[2], Prativa Amom[1], Breana D. Anderson[1], Priya Sivaramakrishnan[2], Shaili D. Patel[2], Barrington Alexander Bennett[2], Teddy D. Lavon[2], Felicia Peng[2], Amanda L. Zacharias[1,3,4]

1. **Division of Developmental Biology, Cincinnati Children's Hospital Medical Center, Cincinnati, OH 45229**
2. **Department of Genetics, Perelman School of Medicine, University of Pennsylvania, Philadelphia, PA 19104**
3. **Department of Pediatrics, University of Cincinnati College of Medicine, Cincinnati, OH 45267**
4. **Corresponding author - *Amanda.Zacharias@cchmc.org***

Abstract

Hox transcription factors play a conserved role in specifying positional identity during animal development, with posterior Hox genes typically repressing the expression of more anterior Hox genes. Here, we dissect the regulation of the posterior Hox genes *nob-1* and *php-3* in the nematode *C. elegans*. We show that *nob-1* and *php-3* are co-expressed in gastrulation-stage embryos in cells that previously expressed the anterior Hox gene *ceh-13*. This expression is controlled by several partially redundant transcriptional enhancers. Surprisingly, these enhancers require *ceh-13* for expression, providing an example of an anterior Hox gene positively regulating a posterior Hox gene. Several other regulators including *elt-1/GATA*, *ceh-20/ceh-40/Pbx*, *unc-62/Meis*, *pop-1/TCF*, *ceh-36/Otx* and *unc-30/Pitx* also act positively through *nob-1/php-3* enhancers. We identified defects in both cell position and cell division patterns in *ceh-13* and *nob-1;php-3* mutants, suggesting that these factors regulate lineage identity in addition to positional identity. Taken together, our results highlight the complexity and unexpected flexibility of Hox gene regulation and function.

Introduction

Hox genes are conserved transcription factors famously expressed in specific positions along the anterior-posterior axis during animal development that specify axial position. Mutations in Hox genes cause a wide variety of developmental defects in both model organisms and humans. Hox gene regulation is complex, and includes both transcriptional and post-transcriptional control. In most animals, Hox genes are found in genomic clusters, and their expression along the A-P axis is collinear with their genomic position, and often show "posterior dominance," where posterior Hox genes repress the expression of more anterior Hox genes (Reviewed in [1–3]).

The genome of the nematode *Caenorhabditis elegans* encodes a single set of six Hox genes, loosely organized into three degenerate "clusters" on Chromosome III, each consisting of two adjacent genes[3,4]. In larval stages, these genes are expressed in specific positions along the A-P axis and regulate both positional differences in cell fate and function, similar to their homologs in other animals[5–12], and directly regulate terminal fates[13].

Three of these, the anterior Hox gene *ceh-13/HOX1* and the posterior Hox genes *nob-1/HOX9-13* and *php-3/HOX9-13,* are also expressed in early embryogenesis, during gastrulation[14–17]. *ceh-13* mutants have severe defects in head morphology[16], while mutants lacking both *nob-1* and *php-3* have severe tail defects[14]. Partial cell lineage tracing of *ceh-13* and *nob-1*;*php-3* mutants identified defects in cell position but not in division patterns, leading to the hypothesis that these genes regulate positional identity, rather than lineage identity[4,14,16].

Intriguingly, despite their apparently opposite roles in anterior vs posterior morphogenesis, both *ceh-13* and *nob-1* are expressed in overlapping posterior lineages during gastrulation and both require the Wnt pathway for this expression[18,19]. *ceh-13* is transiently expressed in the progeny of 7 of the 8 posterior sister cells derived from the (largely ectoderm-producing) AB blastomere at the 24-cell stage[15]. *nob-1* is expressed 1-2 cell cycles later, in the posterior daughters or grand-daughters of four of these *ceh-13*-expressing cells[17]. In addition, both *ceh-13* and *nob-1* are expressed in the posterior daughter of the intestinal blastomere E ("Ep"). This raises the question of whether *ceh-13* regulates *nob-1* in these lineages. Expression of both factors at later stages is regulated by feedback mechanisms; early *ceh-13* activity is required for later ceh-13 expression[19], and early *nob-1* negatively regulates later *nob-1* expression through the microRNA *mir-57*[17].

Here we analyze the *cis*-regulatory control of *ceh-13* and *nob-1* expression in the early embryo. We find that nob-1 expression is regulated by several partially redundant distal enhancers, including at least three that drive overlapping patterns during gastrulation. Two of these enhancers are positively regulated by *ceh-13*, while a third appears *ceh-13*-independent. We identify the GATA family transcription factor *elt-1*, previously known as a specifier of epidermal fate, as one of several additional positive regulators of *nob-1* expression. Detailed analysis of cell positions and cell division timing identifies both position and cell cycle defects in *ceh-13* and *nob-1*/*php-3* mutants. This positive regulation of a posterior Hox gene by an anterior Hox gene suggests a novel role of Hox genes in early lineage specification.

Results

The anterior Hox gene *ceh-13* and the posterior Hox gene *nob-1* are expressed sequentially in gastrulating embryos

We first determined when and in which embryonic cells *ceh-13* and *nob-1* are expressed (Figure 1). To do this, we collected 3D timelapse movies (~1.5 minute temporal resolution) of embryos expressing either *ceh-13, nob-1* or *php-3* tagged with GFP at their C-termini at the endogenous locus by CRISPR/Cas9 genome editing. The same embryos also expressed a ubiquitously expressed mCherry-tagged histone transgene to allow for cell lineage tracing. We traced cells from soon after fertilization (4-8 cell stage) through the last round of cell divisions for most cells (bean stage) by using StarryNite automated cell tracking software, and quantified reporter expression in each cell across time[20–23].

Consistent with previous studies with shorter reporters, CEH-13 expression is first seen in early gastrulation (26-50 cell stage) in cells derived from eight Wnt-signaled posterior sister cells at the 26-cell stage (early gastrulation) (Figure 1B,C, Supplemental Figure 2). These include the AB lineage-derived cells ABalap, ABalpp, ABarpp, ABplap, ABplpp, ABprap and ABprpp, and the posterior endoderm progenitor Ep. The ABalap and ABalpp expression was very weak and barely detectable, while the other lineages had more robust expression. Later expression was seen in muscle progenitors derived from the D blastomere (Dxaa and Dxpp). Finally, expression began at the 200-350 cell stage in MS lineage progenitors that give rise to body wall and pharyngeal muscle, pharyngeal interneurons and the g1 pharyngeal gland cells, and in the epidermal (hyp7) cells ABp(l/r)aapppp. At this stage, a small subset of the lineages that began expressing at the 26-cell stage sustained or increased their expression (P1/P2/P3/P4/P5/P6/P7/P8, V1/V2/V4/V6, DA, DD and ALM/BDU neuroblasts), whereas most cells from these lineages lost CEH-13 expression (Figure 1D). We compared the reporter expression pattern to that of the endogenous mRNA as measured in a lineage-resolved single cell RNA-seq dataset, and found that the mRNA and reporter expression was identical for all cells measured in both datasets[24].

This expression was recapitulated by a rescuing CEH-13::GFP fosmid transgene in which *ceh-13* is tagged at the C-terminus with GFP along with 24 kb of upstream and 7.9kb of downstream sequence (Supplemental Figure 1). The fosmid reporter was brighter than the CRISPR reporter (presumably due to higher copy number), making it easier to detect the weak expression in the ABalap and ABalpp, and had additional weak expression in epidermal precursors from the C lineage (Cxaaa/Cxaapa/Cpapap) not seen in the CRISPR line. We also analyzed a shorter reporter containing only 8.2kb of upstream sequence. This reporter drove similar expression to the longer reporters but did not drive expression in the MS lineage or in the AB derived cells hyp7 and P1/2, emphasizing the important role of distal regulatory elements in regulating *C. elegans* Hox gene expression[25,26].

We defined the embryonic expression patterns of the posterior Hox genes *php-3* and *nob-1* by imaging strains in which each gene is tagged with GFP at the endogenous locus by CRISPR genome engineering. *nob-1* and *php-3* are adjacent in the genome with *php-3* directly downstream of *nob-1*, and are expressed in identical patterns in both our GFP imaging data (Supplemental Figure 1A) and in the single-cell RNA-seq data[24]. NOB-1/PHP-3 expression begins during mid-gastrulation in cells derived from the cells ABplapp, ABplppp, ABprapp, ABprppp, Ep, and the four posterior great-granddaughters of the C blastomere. Expression becomes stronger one cell cycle later in the ABplapap/ABplappp/ABprapap and ABprappp lineages. Later embryonic expression occurs in the ABp(l/r)papppp lineages starting at the onset of morphogenesis ("bean" stage). NOB-1::GFP expressing lineages give rise to fates including neurons, hypodermis, seam cells, epithelial cells, intestine, and death, and have posterior positions clustered in and near the developing tail at comma stage. Similar to CEH-13, early NOB-1::GFP expression persists through the terminal cell divisions in only a subset of cells (Figure 1D). A previously described rescuing NOB-1::GFP transgene that includes 9kb of sequence upstream of the *nob-1* transcript expresses GFP in a similar pattern, except it is not expressed in the C great-granddaughter lineages, suggesting this expression requires regulatory sequences outside of this region[17] (Figure 1D, Supplemental Figure 1).

Early CEH-13::GFP expression occurs in cells that are distributed broadly along the anterior-posterior axis (Figure 1B). Initial NOB-1::GFP expression is more limited to the posterior of the embryo, and in the AB lineage occurs in cells that were the posterior sister after cell division and whose mother expressed CEH-13::GFP one cell cycle earlier (Figure 1D-H). In

addition, the genes are co-expressed at similar onset times in the posterior intestine lineage derived from Ep. In contrast, in late embryos, high levels of CEH-13::GFP and NOB-1::GFP are mutually exclusive, consistent with classic models of Hox expression and posterior dominance.

Several overlapping lineage specific enhancers regulate *nob-1* embryonic expression

To allow us to identify regulators of *nob-1* embryonic expression, we tested nearby genomic sequences for *cis*-regulatory activity in the embryo (Figure 2A,B). Previous work showed that other *C. elegans* Hox genes are regulated by distal enhancers located as much as 20kb from a given gene's promoter[19,25,27], but enhancers for *nob-1* and *php-3* have not been identified.

We took advantage of a series of existing reporters of different lengths to narrow the sequence search space for *nob-1* embryonic enhancers (Figure 2C). A transcriptional reporter containing just 5.3 kb of upstream sequence driving histone-mCherry reporter expression, and the rescuing 9kb NOB-1::GFP reporter are expressed in most of the same lineages as endogenous NOB-1::GFP, indicating they contains sequences sufficient for expression in full set of expressing lineages. However, while the protein fusion reporters are expressed at similar levels in each lineage, the shorter 5.3kb transcriptional reporter has much lower expression in the ABp(l/r)ppp lineages compared to other expressing lineages (Figure 2C). This suggests that additional sequences between -5.3kb and -9kb are required for the full endogenous expression levels in ABp(l/r)ppp.

Other *Caenorhabditis* species including *C. briggsae*, *C. remanei*, *C. japonica* and *C. brenneri* share with *C. elegans* a large (12-20kb) intergenic region upstream of *nob-1*. While the maintenance of such a large intergenic region across evolution could be due to conserved regulatory functions, there is no detectable sequence conservation in the 5.3kb region upstream of *nob-1*, and only two short conserved stretches (85 and 275 nucleotides long) between 5.3 and 9kb upstream. This suggests that any conserved regulatory elements in this region have diverged substantially at the sequence level during *Caenorhabditis* evolution.

Chromatin marks typically used to identify transcriptional enhancers such as H3K27ac, H3K4me, or chromatin accessibility from whole embryos[26,28,29] did not show strong peaks near *nob-1* or near 20 additional genes expressed in lineage-specific patterns at the same stage as *nob-1*[30]. We hypothesized that these signals are diminished in early embryos because the experiments used embryos of mixed stages where later stage nuclei dramatically outnumber nuclei from earlier stages.

We searched for other factors with published genomic binding patterns that could mark embryonic enhancers. One pattern stood out as preferentially bound near early-expressed genes: embryonic binding of a NHR-2::GFP fusion protein[31,32]. NHR-2::GFP binds in the intergenic sequences upstream of 19 of these 20 genes, and 16 genes have multiple clustered NHR-2 binding sites (vs. 22% and 8% of randomly chosen genes, respectively, $p < 0.001$; chi-squared test). NHR-2 is a nuclear hormone receptor distantly related to mammalian thyroid and PPAR receptors, and NHR-2::GFP is expressed in most or all somatic cells from the ~50-cell to ~200-cell stages. The functional importance of NHR-2 binding is unclear; *nhr-2* RNAi causes embryonic and larval arrest, but partial deletion alleles are viable. However, regardless of its function, we hypothesized that these clustered NHR-2 binding sites might be useful proxies for accessible chromatin and could predict enhancer activity in the early embryo.

We tested four NHR-2::GFP-bound regions upstream of *nob-1* (Figure 2A) for enhancer activity by generating transgenic worms expressing histone-mCherry under the control of each candidate enhancer placed upstream of a *pes-10* minimal promoter(Figure 2B) which drives no consistent embryonic expression on its own. We also tested three additional sequences for which we observed no NHR-2::GFP binding but which contained putative binding motifs for POP-1/TCF, which is required for expression of the *nob-1* transcriptional reporter [cite Zacharias]. We identified embryonic cells expressing each enhancer reporter by confocal time lapse imaging and StarryNite. Three of the regions (-3.4kb, -4.3kb and -8.3kb) tested showed enhancer activity that was consistent between embryos and also overlapped with the endogenous NOB-1::GFP expression pattern, suggesting they represent functional enhancers (Figure 2C, Supplemental Figure 2).

The -3.4kb enhancer recapitulates most of the *nob-1* early embryonic expression pattern including in ABp(l/r)app, ABp(l/r)ppp and Ep; with some differences in the C sublineage. This enhancer drives much weaker expression in ABp(l/r)ppp than in ABp(l/r)app, similar to the *nob-1* -5.3 kb upstream transcriptional reporter. The -4.3kb enhancer also drives expression in ABp(l/r)app and ABp(l/r)ppp, but with similar levels of expression. However when this -4.3 kb enhancer was cloned downstream of the reporter, expression was weaker in ABp(l/r)ppp compared to ABp(l/r)app, more closely matching the full transcriptional reporter. We also observed variable misexpression in cells that don't normally express NOB-1 when the -4.3kb enhancer was located adjacent to the promoter. This confirms the -4.3kb region as a *bona fide* enhancer capable of acting at a distance, and suggests that the placement of this enhancer relative to the promoter influences its activity differently in different lineages, and may be important for specificity. Consistent with its ability to bind regulators of *nob-1/php-3*, embryos carrying multiple copies of the -4.3 kb enhancer occasionally displayed the "no backend" phenotype observed in *nob-1/php-3* mutant embryos[14] (Supplemental Figure S2). A third *nob-1* enhancer (-8.3kb) drives early embryonic expression only in ABp(l/r)ppp, as well as later expression in ABp(l/r)papppp. This most-upstream enhancer is included in -9kb NOB-1::GFP transgene but not the shorter -5.3kb transcriptional reporter, and includes the only substantial stretch of conserved sequence in the *nob-1* promoter region. This region thus potentially explains why ABp(l/r)ppp expression is relatively stronger in the translational reporter compared to the shorter transcriptional reporter.

The remaining four enhancer candidates drove no consistent early embryonic expression. It is worth noting that because some *C. elegans* transcripts, including *nob-1*, undergo trans-splicing at their 5' end, the end of the transcript may not represent the site of transcription initiation. Indeed cap-based sequencing approaches indicate that the most likely *nob-1* transcription start site is 693 base pairs upstream of the 5' transcript end. Intriguingly, two enhancer candidates we tested that correspond to the presumptive core promoter (-310bp enhancer) and 'outron' (-84bp enhancer) drove weak and variable expression, with different early embryonic lineages expressing the reporter in different embryos. The sequences between the -3.4kb and -4.3kb enhancers (-3.8 region) also drives variable expression not seen in the full-length reporters. Finally, the -1.3kb region drives late expression in muscle cells after the onset of morphogenesis. This suggests these regions may have broad or non-specific regulatory activity that is restricted to the appropriate cells by other nearby sequences.

As the -5.3kb *nob-1* transcriptional reporter includes both the -3.4kb and -4.3kb enhancers, we deleted each enhancer from this construct to test their necessity for *nob-1* expression (Figure 2C). Deleting both enhancers led to a complete loss of early embryonic

expression in both AB sublineages, suggesting there are no additional enhancers sufficient for early embryonic expression in these regions. The deletion of the -3.4 kb enhancer did not disrupt expression in ABp(l/r)app, ABp(l/r)ppp and in the absence of the -4.3 kb enhancer, this enhancer was not sufficient to rescue expression in these sublineages. This indicates that while this enhancer may be sufficient to drive expression when placed directly next to the promoter, it is unable to drive expression in the endogenous context. Conversely, the -4.3 kb enhancer is a key driver of expression in these sublineages. Additional sequences that drive the expression in the Ep and Cpapp sublineages must exist within the -5.3 kb upstream region.

ceh-13 **and Hox cofactors activate** ***nob-1*** **expression**

Because *ceh-13* expression precedes that of *nob-1* in many lineages, we asked whether *ceh-13* is required for *nob-1* expression. To evaluate this, we examined *nob-1* reporter expression in embryos homozygous for a *ceh-13* null mutation [cite Brunschwig et al]. Expression of the *nob-1* transcriptional reporter is eliminated in ABp(l/r)ppp (p=0.001), and decreased by 25% in ABp(l/r)ap, and 40% in Ep (p=0.02) (Figure 3A-C). Depletion of *ceh-13* by RNAi gave similar results with the transcriptional reporter (p=0.002). In contrast, *ceh-13* RNAi does not significantely alter expression of the -9kb NOB-1 protein reporter, indicating that the additional regulatory sequences in this reporter render it robust to loss of *ceh-13* (Supplemental Figure 3A).

To determine which enhancers require *ceh-13*, we measured the activity of individual *nob-1* enhancer reporters in worms lacking *ceh-13* (Figure 3A, Supplemental Figure 3A). In *ceh-13* mutants, expression driven by the -3.4 kb enhancer decreased significantly in all expressing cells, excluding the C lineage (p=0.003) with an average decrease of 90% and complete loss in ABp(l/r)ppp. *ceh-13* loss also reduces activity of the -4.3 kb enhancer in ABp(l/r)ppp (47% decrease) but expression in ABp(l/r)ap is unchanged. This indicates that other factors besides *ceh-13* activate this enhancer in ABp(l/r)ap and suggests that this enhancer may be responsible for the residual expression of the 5.3kb transcriptional regulation in this lineage in *ceh-13* mutants. The distal -8.3kb enhancer also lost expression in ABp(l/r)ppp (p=0.047), indicating its activity also requires *ceh-13*. Motif analysis identified six putative *ceh-13*-binding motifs in the -3.4kb enhancer; mutating these sites abolished expression in the AB and C lineage ($p<0.02$, $p<0.03$), but did not alter expression in the Ep lineage (Figure 3A, Supplemental Figure 3B). Together, our results show that multiple *ceh-13*-dependent enhancers work together to regulate *nob-1* expression in gastrulating embryos.

Expression of classically defined Hox targets often require Hox cofactors such as *homothorax* or *extradenticle*. These cofactors help Hox TFs bind DNA and can provide additional specificity, and may also have Hox-independent functions[33–35]. To determine when and where Hox cofactors are expressed in early embryos, we used StarryNite to trace the expression of translational reporters for *unc-62*, the *C. elegans homothorax/Meis* homolog, and of *ceh-20* and *ceh-40*, the homologs of *extradenticle/Pbx*. A third *extradenticle* homolog, *ceh-60*, is only expressed in later development (>200 minutes) and does not overlap with *ceh-13*, so was not investigated further[24]. We found that each of these genes has specific and dynamic expression patterns that are highly overlapping with each other and with *ceh-13* and *nob-1* expression (Figure 4A-D, Supplemental Figure 5). In particular, all three cofactors are coexpressed with CEH-13 in cells that will later express NOB-1. Other CEH-13 and NOB-1 expressing cells also express all three cofactors, except only CEH-20 is expressed in the early E lineage, and all three are lost in the NOB-1-expressing ABp(l/r)appp lineage as the embryo

approaches morphogenesis. We conclude that Hox cofactors are expressed in cells where *ceh-13* activates *nob-1* expression.

We tested whether Hox cofactors regulate *nob-1* expression by examining *nob-1* reporter expression after loss of each gene. Depleting *unc-62* by RNAi led to significant loss of expression of the *nob-1* -5.3kb reporter in all AB sublineages (80% decrease, p=0.001), with near complete loss in the ABp(l/r)apap and ABp(l/r)ppp sublineages (Figure 4E). The -9kb NOB-1:GFP protein reporter showed similar expression decreases, although this was only significant in ABp(l/r)appa and incompletely penetrant in other lineages (Supplemental Figure 4B-C). In contrast, CEH-13::GFP reporter expression was unchanged after *unc-62* RNAi (Supplemental Figure 4D). These results show that *nob-1* is regulated by *unc-62*. The fact that *unc-62* RNAi has a stronger phenotype in ABp(l/r)appa than loss of *ceh-13* suggests that *unc-62* may regulate *nob-1* independently of *ceh-13* in these cells.

To investigate the role of the *extradenticle* homologs, we examined the *nob-1* transcriptional reporter in a *ceh-40(gk159)* null mutant background in embryos of worms treated with control or *ceh-20* RNAi. We found *ceh-20* RNAi caused a significant loss of expression in virtually all expressing cells including Ep and Cpap as compared to control RNAi (97% decrease, p<0.004). Some significantly reduced expression remains in ABp(l/r)ap (96% decrease, p<0.004) (Figure 4D).This indicates that the *exd* homologs *ceh-20* and *ceh-40* are required to activate nob-1 and that they are at least partially independent of *ceh-13* in the ABp(l/r)ap, Ep, and Cpap sublineages. This finding is consistent with previous reports that *nob-1* and *ceh-40* have a synthetic lethal genetic interaction[36].

Multiple lineage-specific embryonic TFs including *elt-1/GATA*, *ceh-36/OTX* and *unc-30/PITX* are required for early *nob-1* expression

Since some NOB-1::GFP reporter expression remains in the absence of *ceh-13*, especially in the ABp(l/r)ap lineage, other factors must also activate *nob-1* in these cells. Indeed, we previously identified the Wnt effectors *pop-1* and *sys-1* as activators of *nob-1* expression[18]. We took advantage of the distinct expression patterns of the nob-1 enhancers, as well as databases of TF expression, to search for additional regulators.

Only two of the three enhancers (-3.4kb and -4.3kb) drive expression in the ABp(l/r)ap sublineage, and this expression is less dependent on *ceh-13* than expression in the ABp(l/r)pp lineage. To identify regulators of *nob-1* in this lineage, we searched for TFs expressed specifically in ABp(l/r)ap, and that have predicted binding motifs in the -3.4kb and -4.3kb enhancers[30,37,38]. The GATA Zinc finger encoded by *elt-1* emerged as a candidate. An ELT-1::GFP reporter is expressed prior to gastrulation in the ABp(l/r)ap progenitors ABpla and ABpra, in the other major epidermis-producing lineages ABarp, Caa and Cpa, and in the primarily neuronal lineages ABalap and ABalppp (Figure 5A). ELT-1::GFP expression in the ABpla/ABpra lineages could be detected at least 20 minutes prior to *nob-1* reporter expression in ABp(l/r)ap (Figure 5B). GATA Motifs predicted to bind ELT-1 are enriched in the ABp(l/r)ap enhancers -3.4kb (8 sites) and -4.3kb (7 sites) enhancers compared to the -8.3 enhancer (1 site), which does not drive expression in ABp(l/r)ap.

To test whether *elt-1* regulates *nob-1* expression, we measured the activity of *nob-1* reporters in the *elt-1(ok1002)* null mutant background (Figure 5E-G, Supplemental Figure 6A,B). We found that *elt-1* mutants showed significantly decreased expression of the transcriptional

reporter in the ABp(l/r)ap lineage (87% decrease, p=0.014), and the C(a/p)ap lineage (92% decrease), in which *elt-1* precedes *nob-1* expression, but not in ABp(l/r)pp, where ELT-1::GFP is not expressed. Similarly, we observed decreases in the same sublineages for the -3.4kb enhancer reporter (ABp(l/r)ap: 72% decrease, p=0.008; C: 71% decrease, p=0.03) and the -4.3kb enhancer reporter (ABp(l/r)ap: 31% decrease). To determine if elt-1 was directly regulating the -3.4kb enhancer we mutated the predicted ELT-1 binding sites, which have a characteristic GATA motif. This caused a loss of reporter expression in all lineages (p=0.001). We conclude that *elt-1* activates *nob-1* expression in the ABp(l/r)ap lineage through at least two enhancers, and is at least partially redundant with other factors that may bind GATA motifs.

We previously showed that two homeodomain family TFs, *ceh-36/OTX* and *unc-30/PITX* are redundantly required for proper development of the ABp(l/r)p lineage[39]. Since *ceh-13* and *elt-1* mutants still have some *nob-1* reporter expression in the ABp(l/r)p descendants, we hypothesized that *ceh-36* and *unc-30* might be important for *nob-1* expression in these lineages. To test this, we examined NOB-1::GFP expression in *ceh-36;unc-30* double mutant embryos, and found that two of eight embryos lost expression in this lineage (Supplemental Figure 7A). Furthermore, the ratio of ABp(l/r)ap to ABp(l/r)ppp expression significantly increased (p=0.002) in the remaining double mutant embryos, consistent with a decrease in ABp(l/r)ppp expression (Supplemental Figure 7B). In conclusion, at least seven partially redundant lineage specific transcription factors positively regulate *nob-1* expression: *ceh-13, ceh-20, ceh-40, unc-62, elt-1*, *ceh-36* and *unc-30*.

ceh-13 and nob-1 are required for correct cell position and division patterns in the early embryo

Previous work suggested that *nob-1* and *ceh-13* are required for cell position but not other aspects of cell fate specification[14]. However, mutating lineage identity regulators often leads to cell cycle defects[39,40] that could have been missed in previous studies. To test for such defects, we measured cell positions and cell division timing in six *nob-1* and *ceh-13* mutant embryos by time-lapse microscopy and StarryNite cell tracking, and compared them to a database of 17 wild type embryos[22,39]. (Figure 6)

Consistent with previous work[14], we observed striking global patterns of cell position defects in *nob-1* mutant embryos. The most severe and highest penetrance defects were in cells from NOB-1-expressing lineages (Figure 6A,C,D,G, Supplemental Figure 8)). In total, 48% (62 of 127) of cells descended from NOB-1::GFP expressing lineages had severe position defects (>5 micron deviation, z score > 3.5) in at least two embryos compared to 1.2% (14 of 1094) of cells from non-expressing lineages ($p << 10^{-20}$). However, a large number of cells from non-expressing lineages were moderately mis-positioned, suggesting that many defects are not cell-autonomous. Globally, dorsal cells that normally express NOB-1 fail to migrate to the posterior at 230 minutes post-fertilization; by 300 minutes non-expressing ventral cells compensate by inappropriately moving to the posteriorly, resulting in a global counterclockwise rotation of cell positions when the embryo is viewed from the left aspect (Figure 6G).

We also identified broad cell position defects in *ceh-13* mutant embryos (Figure 6B,E,F,H). Intriguingly, the global patterns of cell position defects differed from *nob-1* mutants. The number of severe position defects was lower for *ceh-13* than for *nob-1*, with 4% (15/357) of cells descended from CEH-13::GFP expressing lineages severely displaced in at least two embryos, as opposed to 0.5% (5/874) of cells from non-expressing lineages ($p << 10^{-20}$). At 210 minutes, (200 cell stage), the most strongly mispositioned cells were *ceh-13*-expressing but *nob-1* non-expressing cells in the posterior ventral region of the embryo. At this stage, cells on

the dorsal surface were posteriorly mispositioned, such that cells in the posterior half of the embryo were rotationally mispositioned clockwise, the opposite direction to that seen in *nob-1* mutants (Figure 6H). Cells at the anterior ventral surface (both *ceh-13*-expressing and non-expressing) were mispositioned towards the posterior, resulting in a counterclockwise rotational defect in the anterior half of the embryo. At later stages, these global defects were largely resolved, and after the onset of morphogenesis the position defects were largely limited to a small number of strongly mispositioned cells. The most extreme were the DA and SAB motorneurons after 300 minutes (bean stage), which were mispositioned several cell diameters anterior of their wild-type position.

In contrast to previous studies, we also identified numerous cell cycle defects in both *nob-1* and *ceh-13* mutants, and these were also heavily restricted to expressing lineages (Figure 6A,B). 13% of *nob-1* expressing cells and 5% of *ceh-13* expressing cells had severe cell division timing defects in at least two of the corresponding mutant embryos (>5 minute deviation from wild type, and z-score >5), vs none in non-expressing cells ($p << 10^{-20}$). The most common cell cycle defect in *nob-1* mutants was the PLM/ALN neuroblast mother (ABp(l/r)apappp), which failed to divide in 8 of 12 observations (Figure 6I). The neuroblast that produces the PHA, PVC and LUA neurons instead underwent programmed cell death in two of 12 mutant lineages. Other cells had multiple cell cycle delays including the PVQ neuroblast, PHB/HSN neuroblast, and the mother of the epidermal cells PHsh, hyp8 and hyp9. All of these cells also were mispositioned (mean 5 micron deviation from expected position). The most striking defects in *ceh-13* mutants were in the cells ABarppaaa(a/p), which normally differentiate into the ADE sheath (glial) cell and H2 epidermal cell, but instead each divided inappropriately in 4 of 6 mutant embryos (Figure 6J). In addition, ABplppaaap, which normally undergoes programmed cell death, instead divided in 2 mutant embryos. Several neuroblasts including those producing the DA, DD and SAB motorneurons also had cell division delays. We conclude that both *ceh-13* and *nob-1* are required not only for proper cell positioning, but also for normal division patterns, suggesting a broader role in fate specification.

Discussion

Classic work defined the concept of Posterior Dominance, in which posterior Hox genes repress the expression and activity of more anterior Hox genes[1]. Indeed, previous work in later developmental stages showed that *nob-1* represses *ceh-13* in the posterior ventral nerve cord[35], consistent with posterior dominance. In contrast, we show that *ceh-13* activates *nob-1/php-3* expression through at least two enhancers during *C. elegans* gastrulation. To our knowledge, this is the first example of an anterior Hox gene positively regulating the expression of a posterior Hox gene during development. *ceh-13* and *nob-1/php-3* are also expressed at an earlier phase in development (pre-gastrulation for *ceh-13* and mid-gastrulation for *nob-1/php-3*) than in many other organisms. Since *C. elegans* is an unsegmented organism, this may have enabled these Hox genes to be co-opted to play earlier “lineage identity” roles in development than is typical for genes in the cluster. This demonstrates an unexpected flexibility in the Hox cluster.

Several studies have highlighted that conserved transcription factors often “moonlight,” with the same factor playing apparently distinct roles in early progenitors and in terminal cell types. For example, the OTX homeodomain TF *ceh-36*, and the PITX homeodomain TF *unc-30*, which both specify specific terminal neuron types, separately act redundantly 6-7 cell divisions earlier in the ABp(l/r)p lineages to specify broad features of lineage identity[39,41–43], and *skn-1*, which is required maternally to specify the endomesodermal blastomere EMS at the 4-cell stage is required postembryonically for oxidative stress resistance and longevity[44,45]. Our work shows

that *ceh-13* and *nob-1/php-3* are another example of this phenomenon. While these were previously shown to regulate positional differences between cells, our identification of cell division defects in each mutant demonstrates they also play a role in lineage specification. Previous work showed that at least one neuron (the PLM touch receptor) is defective in less severe *nob-1* mutants[13]; our work shows that the PLM neuroblasts do not divide normally in *nob-1/php-3* mutants, indicating a function in PLM progenitor lineages. Similarly, *ceh-13* mutants have cell division defects, and *ceh-13* is required for the lineage-specific activity of specific *nob-1* enhancers. Finally, while *elt-1* has a well-defined known role in epidermal fate specification[46], our work shows that it is also required for *nob-1* enhancer activity. This is consistent with other recent work identifying defects in cell division patterns and the expression of the neurogenic TF *lin-32* in *elt-1* mutants[47]. The ability of developmental transcription factors to "moonlight' is likely facilitated by complex regulation by multiple enhancers as seen for *nob-1/php-3*, and *ceh-13*[25,26] since enhancer evolution can enable genes to be expressed at different locations and times in development[48,49].

While early reporter studies found that the expression of many genes expressed in terminal cells is well approximated using just the promoter-proximal region[50], open chromatin mapping studies have identified many distal regions of open chromatin, many of which can act as enhancers[26,28,29]. Our work reinforces these studies and emphasizes the importance of enhancers in *C. elegans* gene regulation. Intriguingly, other genes expressed in lineage-specific patterns around the same time as *nob-1* have similar tendency to have multiple nearby regions of NHR-2::GFP binding and lineage-specific accessible chromatin as measured by ATAC-seq[51], suggesting they may also be regulated by multiple distal enhancers. This could reflect these genes' need for more complex regulation. The *nob-1/php-3* locus contains at least two or three enhancers responsible for expression in each expression domain during gastrulation. This is reminiscent of so-called "shadow enhancers" identified in other organisms, for which redundancy appears to confer robustness in the face of environmental variability[52–54]. This high level of redundancy also appears to extend to the number of transcription factors regulating each enhancer. Current data implicate at least eight TFs as activators of *nob-1* enhancers including *ceh-13*, *elt-1*, *ceh-36*, *unc-30*, the Wnt effector *pop-1*, and the Hox co-factors *ceh-20*, *ceh-40* and *unc-62*. In some cases, the same binding motif may be regulated by different factors in different lineages. For example, mutating six GATA motifs in the -3.4 kb enhancer caused the loss of expression in ABp(l/r)ap, potentially due to loss of ELT-1 binding. However, this mutant also lost expression in Ep, which does not express *elt-1*, but which does express other GATA factors with similar binding specificity including *end-1*, *end-3*,and *elt-7*[55]. In sum, multiple modes of regulatory redundancy could provide a mechanism for the remarkable developmental robustness observed in *C. elegans.*

Methods

<u>Strain generation and propagation</u>

Worm strains (Supplemental Table 1) were maintained at 21-23°C on OP50 *E. coli* on NGM plates. Enhancer reporter strains were generated by injection into RW10029, a GFP histone strain used for lineage tracing. Injection cocktails consisted of reporter DNA construct at 10ng/µL, with 5 ng/µL myo-2p::GFP and 135 ng/µL pBluescript vector and were injected using a Narishige MN-151 micromanipulator with Tritech microinjector system. The *nob-1* promoter deletion strains were generated by injection and compared to a wildtype *nob-1* promoter strain created by injection of pJIM20::nob-1, JIM518. The *ceh-13* rescuing fosmid, *ujIs153*, was created by bombardment of WRM0622C_C06[56] as previously[39]. Other strains were created

through crosses using standard approaches. Lethal alleles were maintained as balanced heterozygotes (*ceh-13(sw1)* or rescued by free duplications (*nob-1(ct223)*), with homozygous mutants recognized by characteristic high-penetrance morphology defects. Lethal *ceh-36;unc-30* double mutants were maintained as homozygotes rescued by an extrachromosomal array carrying *ceh-36*::GFP; lack of rescue was scored by absence of GFP in the ABpxpa lineage. CEH-13::GFP and NOB-1::GFP CRISPR knock-in alleles were created under contract by SUNY Biotech (Fuzhou, China).

Molecular biology

Candidate enhancers were amplified with Phusion HF polymerase (New England Biosciences) from either pJIM20::nob-1 or N2 genomic DNA, with overhangs for stitching, which where then either gel or PCR purified (Qiagen). Putative enhancers were attached to a *pes-10* minimal promoter::HIS-24::mCherry::let-858 3'UTR fragment amplified from POPTOP plasmid[57] (Addgene #34848) by using PCR stitching to create an enhancer reporter which was sequence verified and purified with a PureLink PCR purification kit (ThermoFisher) for injection. The *pes-10* minimal promoter drives no consistent early embryonic expression alone, but has previously been shown to facilitate expression driven by different enhancers[57–59]. For the downstream enhancer experiment, the -4.3kb enhancer was cloned immediately downstream of the stop codon. Tested enhancer sequences can be found in Supplemental Table 2. Putative transcription factor binding sites were identified using CIS-BP (cisbp.ccbr.utoronto.ca)[37,60] (Supplemental Table 3). DNA fragments with desired mutations were synthesized (Integrated DNA Technologies) and PCR stitched as before.

Imaging/Lineaging

We acquired confocal images with a Leica TCS SP5, Stellaris or Nikon A1RSi resonance scanning confocal microscope (67 z planes at 0.5 µm spacing and 1.5 minute time spacing, with laser power increasing by 4-fold through the embryo depth to account for attenuation of signal with depth). Embryos were mounted in egg buffer/methyl cellulose with 20µm beads as spacers[61] and imaged at 22°C using a stage temperature controller (Brook Industries, Lake Villa, IL). We used StarryNite software to automatically annotate nuclei and trace lineages, and AceTree software to identify and fix any errors from the automated analysis, and quantified reporter expression in each nucleus relative to local background (using the "blot" background correction technique) as previously described[20,21,23,62,63].

Quantitative comparisons

Cell averages of nuclear fluorescence were computed for each cell based on all (typically >20) measurements across its lifetime. For each control condition, the average value of each expressing cell was computed and used to determine the fold change for each control and mutant cell, which were displayed as boxplots using R 3.5.1 (The R Foundation for Statistical Computing). Background-corrected expression values were rounded up to zero if values fell below zero. To determine if changes were significant across the sublineage, the summed expression for each cell and time point in each sublineage was calculated for all control and mutant embryos and the two sets of values were compared using a Wilcoxon Ranked Sum test using R.

Mutant cell position analysis

Cell position defects were identified as previously[39]. Briefly, we corrected for differences in global division rates (which did not differ dramatically from wild-type), and considered divisions as defective/outliers if they deviated from the wild-type cell cycle length by at least five minutes and had a z-score greater than three. Cell positions were corrected for differences in embryo

size and rotation, and considered defective if they deviated from the expected wildtype position by at least five microns, had a z-score greater than five, and a nearest neighbor score greater than 0.8 (defined empirically based on the distribution of wild-type scores).

Acknowledgements

We thank Bob Waterston and Adrian Streit for strains. Some strains were provided by the CGC, which is funded by NIH Office of Research Infrastructure Programs (P40 OD010440). We thank Swati Mundre, Tom Sesterhenn,Yannis Belloucif, Ilona Jileaeva for cloning assistance and technical assistance with lineage tracing and worm genetics. We thank Meera Sundaram for the use of injection equipment and reagents. We thank Stephen Nehrbass for software assistance and Matt Kofron and Evan Meyer at the Confocal Imaging Core at Cincinnati Children's, a Nikon Center of Excellence, for their help with imaging, and Matt Batie for designing and building the cooling stage. This work was supported by NIH grants R35GM127093 (to J.I.M.), R00GM111825 (to A.L.Z.), and F31GM123737 (to J.D.R.).

Figure legends

Figure 1: *ceh-13* and *nob-1/php-3* are expressed broadly in an overlapping pattern in the early *C. elegans* embryo. A) Time lapse images of transgenic *C. elegans* embryos carrying two transgenes, a ubiquitous fluorescent histone to mark all nuclei (shown in green) and a reporter of interest (shown in red), which can be a cis-regulatory element driving a fluorescent histone (transcriptional) or a fluorescently tagged transcription factor protein (translational). Image analysis software identifies nuclei, and quantifies reporter intensity within the nuclei, which can be displayed as a lineage tree colored by expression as in (C). B) 3D projections of nuclei expressing a CEH-13::GFP CRISPR reporter (red), NOB-1::GFP or PHP-3::GFP CRISPR reporter (blue), with overlap shown in magenta, at 120 minutes (50 cell stage), 150 minutes (100 cell stage), and 280 minutes (400 cell stage) post fertilization. NOB-1::GFP and PHP-3::GFP CRISPR reporters were expressed in indistinguishable patterns (Supplemental Figure 1), but PHP-3::GFP was slightly brighter so is shown in the following panels. C) Lineage tree though the 100-cell stage, showing early expression of CEH-13 and PHP-3 CRISPR reporters, colored as in (B). D) Expressing sublineages showing CEH-13 and/or PHP-3::GFP CRISPR reporter expression to 350 minutes of development, colors as in (B). Note that CEH-13::GFP precedes PHP-3::GFP and NOB-1::GFP in all sublineages except ABp(l/r)papppp (asterisk - expression is consistent in ABprpapppp and variable in ABplpapppp). (E-H) Quantitative detail for highlighted sublineages, showing nuclear fluorescence intensity of CEH-13::GFP (fosmid) and NOB-1::GFP transgene reporters across developmental time for the cells leading to ABp(l/r)appaaa (E), ABp(l/r)appppp (F), ABp(l/r)pppppppp (G), and Ep(l/r)p (H). Nuclear fluorescence intensity is in arbitrary units. Grey bars mark cell divisions.

Figure 2: Regions upstream of *nob-1/php-3* can recapitulate its expression pattern. A) Genome browser view of the *nob-1*/*php-3* locus showing the genes (black), candidate enhancers tested (brown), sequence conservation with other nematodes (grey), and NHR-2 ChIP-seq trace (dark blue) from modENCODE[32] and ATAC-seq traces (red:ABa sublineage, green: ABp sublineage) from Charest et al, 2020[51]. B) Schematics of the *nob-1* reporter constructs examined, shown in alignment with (A). Enhancers were primarily tested in an orientation 5' to the *pes-10* minimal promoter, but a downstream orientation was also used for the -4.3 kb enhancer. C) Lineage trees colored to show expression patterns for the various reporters and tested enhancers with relevant reproducible activity, using a rainbow color scale

to increase visible dynamic range. Major expressing sublineages are underlined: ABp(l/r)ap: pink, ABp(l/r)ppp: cyan, Ep: black, Cpapp: orange, ectopic: purple. Note the changes in expression driven by the -4.3 kb enhancer depending on its position relative to the *pes-10* minimal promoter. D) Average nuclear fluorescence values for cells in the ABp(l/r)ap (pink) and ABp(l/r)ppp (blue) sublineages from at least four embryos, shown on a log scale. E) Ratio of expression in average ABp(l/r)ap cell to the average ABp(l/r)ppp cell at the 350 cell stage for at least 4 embryos. F) Lineage trees showing expression driven by the nob-1 -5.3 kb upstream region reporter with the -3.4 and/or -4.3 enhancers are deleted. Sublineages where expression is lost are underlined with colors as in (C).

Figure 3: Expression of cis-regulatory elements upstream of *nob-1* and *php-3* depends on *ceh-13*. A) Fold change in expression level relative to mean wild-type control for *nob-1* promoter and enhancers in *ceh-13* mutant and RNAi conditions. *P* values determined by Wilcoxon Ranked Sum Test. B) Lineage view of wild-type *nob-1* -5.3kb upstream reporter ("promoter") expression in specified sublineages. C) *nob-1* promoter reporter expression in *ceh-13(sw1)* null mutant.

Figure 4: Hox co-factors precede *nob-1* and regulate its expression. A) Lineage trees of NOB-1::GFP expressing sublineages, showing the expression of *ceh-13* (fosmid) and *nob-1* (GFP transgene) reporters, and fosmid GFP transgene reporters for the Hox co-factors, *ceh-20*, *ceh-40* and *unc-62* in the ABp, E, and C sublineages. Color thresholds were adjusted for each gene to show all expressing cells. Highlighted branches are shown in graphs B, C and D. B-D) Average TF reporter nuclear fluorescence intensity across embryos (n >= 2) and for left/right symmetric cells across developmental time for the cells leading to B) ABp(l/r)apapa , C) ABp(l/r)pppaa and D) Cpapp. Fluorescence intensity is in arbitrary units and grey bars mark cell divisions. E) Fold change values for *nob-1* promoter expression in untreated and *unc-62* RNAi treated embryos in the causes significant decreases in *nob-1* promoter expression in specified sublineages. F) Fold change values for *nob-1* promoter expression in *ceh-40(gk159)* mutant embryos treated with *ges-1* (control) or *ceh-20* RNAi in the specified sublineages. *P* values determined by Wilcoxon Ranked Sum Test.

Figure 5: *elt-1* regulates *nob-1* expression in ABp(l/r)ap sublineage. A) Partial lineage trees showing ELT-1::GFP (Green), NOB-1::GFP (Blue) or overlapping (Cyan) expression in the ABp and C sublineages. Arrowheads indicate branches shown in subsequent panels. B-D) Average ELT-1::GFP and NOB-1::GFP nuclear fluorescence intensity (arbitrary units) in cells leading to B) ABp(l/r)apppap (neural fate) C), ABp(l/r)appppa (hypodermal fate), and D) Cpappd (hypodermal fate). Grey bars mark cell divisions. E) Fold change values for the *nob-1* promoter and -3.4 kb and -4.3 kb wild-type or mutated enhancers in the ABp(l/r)ap sublineage in the control and *elt-1(ok1002)* mutant conditions. F-G) Fold-change of *nob-1* reporter intensity in *elt-1(ok1002)* relative to mean wild-type control level in the E) ABp(l/r)pp, F) ABp(l/r)ppp, and G) Cpap lineages. *P* values determined by Wilcoxon Ranked Sum Test.

Figure 6: Cell defects are observed in the posterior of both *ceh-13* and *nob-1* mutant embryos. A) Lineage showing *ceh-13* expression with plots of frequency of cell cycle defects and cell position defects for each cell plotted below. Cells expressing *ceh-13* during their development are highlighted in pink (ABalap and ABalpp, which express very low levels of CEH-13::GFP, are denoted with lighter shading). Cell cycle defects are defined as missed, ectopic or significant change in division timing of at least 5 minutes and cell position defects are defined as significant deviation of at least 5 μm from the positions expected from wild type (see methods) [Cite Richards]. Defects are listed cumulatively for terminal cells, so defect in both a parent and daughter cell would be scored as two defects. B) Lineage showing *nob-1* and *php-3* expression overlap with plots of frequency of cell cycle defects and cell position defects for each cell plotted

below. Cells expressing both *nob-1* and *php-3* are highlighted in cyan on the plots. C, D) Plot of mean deviation in microns vs. mean neighbor score (cite Walton et al) for each cell in the embryo, colored by level of NOB-1::GFP expression, for *nob-1(ct223)* mutant (C) and wildtype (D) embryos. E, F) Plot of mean deviation in microns vs. mean neighbor score for each cell in the embryo, colored by level of CEH-13::GFP expression, for ceh-13(sw1) mutant (E) and wildtype (F) embryos. G) Three-dimensional plot of cell position deviations in the *nob-1(ct223)* mutant at 335 minutes of development. Arrows point from average wildtype location to average mutant location for each cell, colors indicate the level of NOB-1::GFP expression. H) Three-dimensional plot of cell position deviations in the *ceh-13(sw1)* mutant at 322 minutes of development, with arrow colors indicating the level of CEH-13::GFP expression. I) Wildtype and *nob-1(ct223)* mutant sublineages for the ABp(l/r)ap and ABp(l/r)pp sublineages, showing examples of cell division defects. Green stars indicate the normal divisions of neuroblasts, orange Xs indicate the failed divisions of these cells with the frequency observed noted below. Blue underline indicates the expression of NOB-1::GFP. J) Wildtype and *ceh-13(sw1)* mutant sublineages for the ABarp sublineage. Green stars indicate the normal development of ADEshL and H2L cells, orange Xs indicate the ectopic division of these cells with the frequency observed noted below. Red underline indicates the expression of CEH-13::GFP.

Supplemental Figure 1: Hox gene are expressed in overlapping patterns. A) Overlap in the expression of NOB-1::GFP and PHP-3::GFP CRISPR knock-in alleles. Expression is nearly identical except *php-3* is expressed more consistently in ABplpapppp. B) Overlap of a CEH-13::GFP fosmid translational reporter transgene with a -9kb NOB-1::GFP rescuing translational reporter transgene. The expression patterns are nearly identical to the CRISPR knock-in alleles except the 9kb NOB-1::GFP reporter has reduced expression in the C lineage. C) Correlation between average PHP-3::GFP CRISPR and NOB-1::GFP CRISPR reporters for each cell during embryonic development. D) Correlation between average CEH-13::GFP CRISPR and NOB-1::GFP CRISPR reporters for each cell during embryonic development. Note that no cells express high levels of both proteins. E) Correlation between average CEH-13::GFP and PHP-3::GFP intensity levels for each cell at each (1.5 minute) time point. Note that no cells express high levels of both CEH-13 and NOB-1.

Supplemental Figure 2: Some *nob-1* enhancer constructs drive variable non-specific expression. A) Representative examples showing the expression variability for each of the enhancers tested. Colored lines indicate the sublineages of interest. Some sublineages with no expression are shown as partial trees. B) Brightfield image of a hatched L1 larva carrying the -4.3kb enhancer reporter and showing the “no backend” phenotype characteristic of *nob-1/php-3* mutants. Nearby bead is 20µm in diameter.

Supplemental Figure 3: *ceh-13* regulates enhancers of *nob-1*. A) Graphs showing the effect of *ceh-13* RNAi on NOB-1::GFP rescuing transgene as well as the control values for the *nob-1* enhancer reporters (*sw1* mutant values same as reported in Fig. 3). Red * indicates $p<0.05$ in Wilcoxon Ranked sum test. B) Sublineage trees showing expression changes relative to wildtype for the -3.4kb enhancer with mutated HOX sites.

Supplemental Figure 4: Hox co-factors affect *nob-1* expression in specific sublineages. A) Tree showing effects of *unc-62i* on *nob-1* promoter transcriptional reporter expression in the ABpl sublineage. Lineages with loss of expression are underlined. The ABp(l/r)apap sublineage was most affected in 13/14 lineages tested. B) Trees showing the effect of *unc-62i* on NOB-1::GFP translational reporter expression, with two examples shown. Sublineages affected are underlined. C) Graphs for all embryos tested (eight) for the same sublineages shown in (B). Red * indicates $p<0.05$ in Wilcoxon Ranked sum test. D) Effect of *unc-62* RNAi on CEH-13::GFP

fosmid reporter in sublineages where the two genes are both expressed. No significant changes were detected.

Supplemental Figure 5: Full Lineages for *nob-1* regulators. Full lineages for CEH-20::GFP, CEH-40::GFP, UNC-62::GFP, and ELT-1::GFP, all fosmid translational reporters. All sublineages are shown to at least the 350 cell stage - selected sublineages are shown later to identify additional expression or dynamics.

Supplemental Figure 6: *nob-1* enhancer expression requires *elt-1*. A) Fold change values of *nob-1* enhancers in *elt-1* mutant conditions in the ABp(l/r)ap and Cpap sublineages (if expressed in control). Red * indicates $p<0.05$ in Wilcoxon Ranked sum test. B) Fold change values of *nob-1* enhancers in *elt-1* mutant conditions in the ABp(l/r)ppp and Ep sublineages (if expressed in control) where elt-1 is not expressed. Red * indicates $p<0.05$ in Wilcoxon Ranked sum test. C) Expression of the -3.4 kb enhancer and a version from which all GATA sites have been mutagenized in the ABp, E and C sublineages. Note: the mutagenesis also disrupted one *ceh-20/40* predicted site, two *nob-1* predicted sites, and one *pop-1* predicted site.

Supplemental Figure 7: *ceh-36* and *unc-30* contribute to *nob-1* expression. A) Wildtype and *ceh-36(ok795);unc-30(ok613)* mutant embryos expressing the NOB-1::GFP reporter transgene. Expression is shown in the ABp sublineage at the ~200 cell stage. B) Boxplot showing the ratio of expression in the ABp(l/r)ap lineage to the ABp(l/r)ppp lineage for wildtype and *ceh-36(ok795);unc-30(ok613)* mutant at the 350 cell stage for at least 4 embryos. Red * indicates $p<0.05$ in Wilcoxon Ranked sum test.

Supplemental Figure 8: Defective positions of specific cells in *nob-1* mutants. A) The position of cells that normally express *nob-1* are highlighted in the context of the whole embryo at ~320 minutes (~570 cells, early morphogenesis). As compared to the wild-type average (left), the *nob-1(ct223)* mutant (right) cells are disorganized and displaced anteriorly, particularly ABp(l/r)ppp and some ABp(l/r)app cells (ABp(l/r)appp). B) The positions of the neuroblasts that fail to divide the *nob-1(ct223)* mutant as compared to control (left), showing that these are dramatically mispositioned.

Supplemental Table 1: Strain List.csv

Supplemental Table 2: Tested enhancer sequences.csv

Supplemental Table 3: nob-1_enhancer_motifs.xlsx

References Cited

1. Duboule D, Morata G. Colinearity and functional hierarchy among genes of the homeotic complexes. Trends Genet TIG. 1994 Oct;10(10):358–364. PMID: 7985240

2. Noordermeer D, Duboule D. Chromatin architectures and Hox gene collinearity. Curr Top Dev Biol. 2013;104:113–148. PMID: 23587240

3. Gaunt SJ. Hox cluster genes and collinearities throughout the tree of animal life. Int J Dev Biol. 2018;62(11–12):673–683. PMID: 30604837

4. Aboobaker A, Blaxter M. Hox gene evolution in nematodes: novelty conserved. Curr Opin Genet Dev. 2003 Dec;13(6):593–598. PMID: 14638320

5. Ferreira HB, Zhang Y, Zhao C, Emmons SW. Patterning of Caenorhabditis elegans posterior structures by the Abdominal-B homolog, egl-5. Dev Biol. 1999 Mar 1;207(1):215–228. PMID: 10049576

6. Takács-Vellai K, Vellai T, Chen EB, Zhang Y, Guerry F, Stern MJ, Müller F. Transcriptional control of Notch signaling by a HOX and a PBX/EXD protein during vulval development in C. elegans. Dev Biol. 2007 Feb 15;302(2):661–669. PMID: 17084835

7. Harris J, Honigberg L, Robinson N, Kenyon C. Neuronal cell migration in C. elegans: regulation of Hox gene expression and cell position. Dev Camb Engl. 1996 Oct;122(10):3117–3131. PMID: 8898225

8. Maloof JN, Whangbo J, Harris JM, Jongeward GD, Kenyon C. A Wnt signaling pathway controls hox gene expression and neuroblast migration in C. elegans. Dev Camb Engl. 1999 Jan;126(1):37–49. PMID: 9834184

9. Yu H, Seah A, Sternberg PW. Re-programming of C. elegans male epidermal precursor fates by Wnt, Hox, and LIN-12/Notch activities. Dev Biol. 2010 Sep 1;345(1):1–11. PMCID: PMC3326348

10. Shemer G, Podbilewicz B. LIN-39/Hox triggers cell division and represses EFF-1/fusogen-dependent vulval cell fusion. Genes Dev. 2002 Dec 15;16(24):3136–3141. PMCID: PMC187502

11. Josephson MP, Chai Y, Ou G, Lundquist EA. EGL-20/Wnt and MAB-5/Hox Act Sequentially to Inhibit Anterior Migration of Neuroblasts in C. elegans. PloS One. 2016;11(2):e0148658. PMCID: PMC4749177

12. Tihanyi B, Vellai T, Regos A, Ari E, Müller F, Takács-Vellai K. The C. elegans Hox gene ceh-13 regulates cell migration and fusion in a non-colinear way. Implications for the early evolution of Hox clusters. BMC Dev Biol. 2010 Jul 28;10:78. PMCID: PMC2915959

13. Zheng C, Jin FQ, Chalfie M. Hox Proteins Act as Transcriptional Guarantors to Ensure Terminal Differentiation. Cell Rep. 2015 Nov 17;13(7):1343–1352. PMCID: PMC4654970

14. Van Auken K, Weaver DC, Edgar LG, Wood WB. Caenorhabditis elegans embryonic axial patterning requires two recently discovered posterior-group Hox genes. Proc Natl Acad Sci U S A. 2000 Apr 25;97(9):4499–4503. PMCID: PMC18263

15. Wittmann C, Bossinger O, Goldstein B, Fleischmann M, Kohler R, Brunschwig K, Tobler H, Müller F. The expression of the C. elegans labial-like Hox gene ceh-13 during early embryogenesis relies on cell fate and on anteroposterior cell polarity. Dev Camb Engl. 1997 Nov;124(21):4193–4200. PMID: 9334268

16. Brunschwig K, Wittmann C, Schnabel R, Bürglin TR, Tobler H, Müller F. Anterior organization of the Caenorhabditis elegans embryo by the labial-like Hox gene ceh-13. Dev Camb Engl. 1999 Apr;126(7):1537–1546. PMID: 10068646

17. Zhao Z, Boyle TJ, Liu Z, Murray JI, Wood WB, Waterston RH. A negative regulatory loop between microRNA and Hox gene controls posterior identities in Caenorhabditis elegans. PLoS Genet. 2010 Sep 2;6(9):e1001089. PMCID: PMC2932687

18. Zacharias AL, Walton T, Preston E, Murray JI. Quantitative Differences in Nuclear β-catenin and TCF Pattern Embryonic Cells in C. elegans. PLoS Genet. 2015 Oct;11(10):e1005585. PMCID: PMC4619327

19. Streit A, Kohler R, Marty T, Belfiore M, Takacs-Vellai K, Vigano M-A, Schnabel R, Affolter M, Müller F. Conserved regulation of the caenorhabditis elegans labial/Hox1 gene ceh-13. Dev Biol. 2002;242(2):96–108.

20. Murray JI, Bao Z, Boyle TJ, Waterston RH. The lineaging of fluorescently-labeled Caenorhabditis elegans embryos with StarryNite and AceTree. Nat Protoc. 2006 Nov;1(3):1468–1476.

21. Bao Z, Murray JI, Boyle TJ, Ooi S-L, Sandel MJ, Waterston RH. Automated cell lineage tracing in Caenorhabditis elegans. Proc Natl Acad Sci. 2006 Feb;103(8):2707–2712.

22. Richards JL, Zacharias AL, Walton T, Burdick JT, Murray JI. A quantitative model of normal Caenorhabditis elegans embryogenesis and its disruption after stress. Dev Biol. 2013 Feb 1;374(1):12–23. PMID: 23220655

23. Santella A, Du Z, Bao Z. A semi-local neighborhood-based framework for probabilistic cell lineage tracing. BMC Bioinformatics. 2014 Jun 25;15:217. PMCID: PMC4085468

24. Packer JS, Zhu Q, Huynh C, Sivaramakrishnan P, Preston E, Dueck H, Stefanik D, Tan K, Trapnell C, Kim J, Waterston RH, Murray JI. A lineage-resolved molecular atlas of C. elegans embryogenesis at single-cell resolution. Science. 2019 20;365(6459). PMID: 31488706

25. Kuntz SG, Schwarz EM, DeModena JA, De Buysscher T, Trout D, Shizuya H, Sternberg PW, Wold BJ. Multigenome DNA sequence conservation identifies Hox cis-regulatory elements. Genome Res. 2008 Dec;18(12):1955–1968. PMCID: PMC2593573

26. Ho MCW, Quintero-Cadena P, Sternberg PW. Genome-wide discovery of active regulatory elements and transcription factor footprints in Caenorhabditis elegans using DNase-seq. Genome Res. 2017 Dec;27(12):2108–2119. PMCID: PMC5741056

27. Teng Y, Girard L, Ferreira HB, Sternberg PW, Emmons SW. Dissection of cis-regulatory elements in the C. elegans Hox gene egl-5 promoter. Dev Biol. 2004 Dec 15;276(2):476–492. PMID: 15581880

28. Jänes J, Dong Y, Schoof M, Serizay J, Appert A, Cerrato C, Woodbury C, Chen R, Gemma C, Huang N, Kissiov D, Stempor P, Steward A, Zeiser E, Sauer S, Ahringer J. Chromatin accessibility dynamics across C. elegans development and ageing. eLife. 2018 Oct 26;7. PMCID: PMC6231769

29. Daugherty AC, Yeo RW, Buenrostro JD, Greenleaf WJ, Kundaje A, Brunet A. Chromatin accessibility dynamics reveal novel functional enhancers in C. elegans. Genome Res. 2017 Dec;27(12):2096–2107. PMCID: PMC5741055

30. Murray JI, Boyle TJ, Preston E, Vafeados D, Mericle B, Weisdepp P, Zhao Z, Bao Z, Boeck M, Waterston RH. Multidimensional regulation of gene expression in the C. elegans embryo. Genome Res. 2012 Jul;22(7):1282–1294. PMID: 22508763

31. Niu W, Lu ZJ, Zhong M, Sarov M, Murray JI, Brdlik CM, Janette J, Chen C, Alves P, Preston E, Slightham C, Jiang L, Hyman AA, Kim SK, Waterston RH, Gerstein M, Snyder M, Reinke V. Diverse transcription factor binding features revealed by genome-wide ChIP-seq in C. elegans. Genome Res. 2011 Feb 1;21(2):245–254.

32. Araya CL, Kawli T, Kundaje A, Jiang L, Wu B, Vafeados D, Terrell R, Weissdepp P, Gevirtzman L, Mace D, Niu W, Boyle AP, Xie D, Ma L, Murray JI, Reinke V, Waterston RH, Snyder M. Regulatory analysis of the C. elegans genome with spatiotemporal resolution. Nature. 2014 Aug 28;512(7515):400–405. PMCID: PMC4530805

33. Slattery M, Riley T, Liu P, Abe N, Gomez-Alcala P, Dror I, Zhou T, Rohs R, Honig B, Bussemaker HJ, Mann RS. Cofactor binding evokes latent differences in DNA binding specificity between Hox proteins. Cell. 2011 Dec 9;147(6):1270–1282. PMCID: PMC3319069

34. Abe N, Dror I, Yang L, Slattery M, Zhou T, Bussemaker HJ, Rohs R, Mann RS. Deconvolving the recognition of DNA shape from sequence. Cell. 2015 Apr 9;161(2):307–318. PMCID: PMC4422406

35. Van Auken K, Weaver D, Robertson B, Sundaram M, Saldi T, Edgar L, Elling U, Lee M, Boese Q, Wood WB. Roles of the Homothorax/Meis/Prep homolog UNC-62 and the Exd/Pbx homologs CEH-20 and CEH-40 in C. elegans embryogenesis. Dev Camb Engl. 2002 Nov;129(22):5255–5268. PMID: 12399316

36. Baugh LR, Wen JC, Hill AA, Slonim DK, Brown EL, Hunter CP. Synthetic lethal analysis of Caenorhabditis elegans posterior embryonic patterning genes identifies conserved genetic interactions. Genome Biol. 2005;6(5):R45. PMCID: PMC1175957

37. Weirauch MT, Yang A, Albu M, Cote AG, Montenegro-Montero A, Drewe P, Najafabadi HS, Lambert SA, Mann I, Cook K, Zheng H, Goity A, van Bakel H, Lozano J-C, Galli M, Lewsey MG, Huang E, Mukherjee T, Chen X, Reece-Hoyes JS, Govindarajan S, Shaulsky G, Walhout AJM, Bouget F-Y, Ratsch G, Larrondo LF, Ecker JR, Hughes TR. Determination and inference of eukaryotic transcription factor sequence specificity. Cell. 2014 Sep 11;158(6):1431–1443. PMCID: PMC4163041

38. Mace DL, Weisdepp P, Gevirtzman L, Boyle T, Waterston RH. A high-fidelity cell lineage tracing method for obtaining systematic spatiotemporal gene expression patterns in Caenorhabditis elegans. G3 Bethesda Md. 2013 May 20;3(5):851–863. PMCID: PMC3656732

39. Walton T, Preston E, Nair G, Zacharias AL, Raj A, Murray JI. The Bicoid class homeodomain factors ceh-36/OTX and unc-30/PITX cooperate in C. elegans embryonic progenitor cells to regulate robust development. PLoS Genet. 2015 Mar;11(3):e1005003. PMCID: PMC4349592

40. Boeck ME, Boyle T, Bao Z, Murray J, Mericle B, Waterston R. Specific roles for the GATA transcription factors end-1 and end-3 during C. elegans E-lineage development. Dev Biol. 2011 Oct 15;358(2):345–355. PMCID: PMC4454387

41. Jin Y, Hoskins R, Horvitz HR. Control of type-D GABAergic neuron differentiation by C. elegans UNC-30 homeodomain protein. Nature. 1994 Dec 22;372(6508):780–783. PMID: 7997265

42. Chang S, Johnston RJ, Hobert O. A transcriptional regulatory cascade that controls left/right asymmetry in chemosensory neurons of C. elegans. Genes Dev. 2003 Sep 1;17(17):2123–2137. PMCID: PMC196454

43. Lanjuin A, VanHoven MK, Bargmann CI, Thompson JK, Sengupta P. Otx/otd homeobox genes specify distinct sensory neuron identities in C. elegans. Dev Cell. 2003 Oct;5(4):621–633. PMID: 14536063

44. An JH, Vranas K, Lucke M, Inoue H, Hisamoto N, Matsumoto K, Blackwell TK. Regulation of the Caenorhabditis elegans oxidative stress defense protein SKN-1 by glycogen synthase kinase-3. Proc Natl Acad Sci U S A. 2005 Nov 8;102(45):16275–16280. PMCID: PMC1283458

45. Bowerman B, Eaton BA, Priess JR. skn-1, a maternally expressed gene required to specify the fate of ventral blastomeres in the early C. elegans embryo. Cell. 1992 Mar 20;68(6):1061–1075. PMID: 1547503

46. Gilleard JS, McGhee JD. Activation of hypodermal differentiation in the Caenorhabditis elegans embryo by GATA transcription factors ELT-1 and ELT-3. Mol Cell Biol. 2001 Apr;21(7):2533–2544. PMID: 11259601

47. Ma X, Zhao Z, Xiao L, Xu W, Wang Y, Zhang Y, Wu G, Du Z. Single-Cell Protein Atlas of Transcription Factors Reveals the Combinatorial Code for Spatiotemporal Patterning the C. elegans Embryo. bioRxiv. Cold Spring Harbor Laboratory; 2020 Jul 7;2020.06.30.178640.

48. Carroll SB. Evolution at two levels: on genes and form. PLoS Biol. 2005 Jul;3(7):e245. PMCID: PMC1174822

49. Levine M. Transcriptional enhancers in animal development and evolution. Curr Biol CB. 2010 Sep 14;20(17):R754-763. PMCID: PMC4280268

50. Reece-Hoyes JS, Shingles J, Dupuy D, Grove CA, Walhout AJM, Vidal M, Hope IA. Insight into transcription factor gene duplication from Caenorhabditis elegans Promoterome-driven expression patterns. BMC Genomics. 2007 Jan 23;8:27. PMCID: PMC1785375

51. Charest J, Daniele T, Wang J, Bykov A, Mandlbauer A, Asparuhova M, Röhsner J, Gutiérrez-Pérez P, Cochella L. Combinatorial Action of Temporally Segregated Transcription Factors. Dev Cell. 2020 Nov 23;55(4):483-499.e7. PMCID: PMC7704111

52. Hong J-W, Hendrix DA, Levine MS. Shadow enhancers as a source of evolutionary novelty. Science. 2008 Sep 5;321(5894):1314. PMCID: PMC4257485

53. Frankel N, Davis GK, Vargas D, Wang S, Payre F, Stern DL. Phenotypic robustness conferred by apparently redundant transcriptional enhancers. Nature. 2010 Jul 22;466(7305):490–493. PMCID: PMC2909378

54. Perry MW, Boettiger AN, Bothma JP, Levine M. Shadow enhancers foster robustness of Drosophila gastrulation. Curr Biol CB. 2010 Sep 14;20(17):1562–1567. PMCID: PMC4257487

55. Maduro MF. Gut development in C. elegans. Semin Cell Dev Biol. 2017 Jun;66:3–11. PMID: 28065852

56. Sarov M, Murray JI, Schanze K, Pozniakovski A, Niu W, Angermann K, Hasse S, Rupprecht M, Vinis E, Tinney M, Preston E, Zinke A, Enst S, Teichgraber T, Janette J, Reis K, Janosch S, Schloissnig S, Ejsmont RK, Slightam C, Xu X, Kim SK, Reinke V, Stewart AF, Snyder M, Waterston RH, Hyman AA. A genome-scale resource for in vivo tag-based protein function exploration in C. elegans. Cell. 2012 Aug 17;150(4):855–866. PMID: 22901814

57. Green JL, Inoue T, Sternberg PW. Opposing Wnt pathways orient cell polarity during organogenesis. Cell. 2008 Aug 22;134(4):646–656. PMID: 18724937

58. Fire A, Harrison SW, Dixon D. A modular set of lacZ fusion vectors for studying gene expression in Caenorhabditis elegans. Gene. 1990 Sep 14;93(2):189–198. PMID: 2121610

59. Wei X, Potter CJ, Luo L, Shen K. Controlling gene expression with the Q repressible binary expression system in Caenorhabditis elegans. Nat Methods. 2012 Mar 11;9(4):391–395. PMCID: PMC3846601

60. Narasimhan K, Lambert SA, Yang AWH, Riddell J, Mnaimneh S, Zheng H, Albu M, Najafabadi HS, Reece-Hoyes JS, Fuxman Bass JI, Walhout AJM, Weirauch MT, Hughes TR. Mapping and analysis of Caenorhabditis elegans transcription factor sequence specificities. eLife. 2015 Apr 23;4. PMCID: PMC4434323

61. Bao Z, Murray JI. Mounting Caenorhabditis elegans Embryos for Live Imaging of Embryogenesis. Cold Spring Harb Protoc. Cold Spring Harbor Laboratory Press; 2011 Sep 1;2011(9):pdb.prot065599. PMID: 21880814

62. Boyle TJ, Bao Z, Murray JI, Araya CL, Waterston RH. AceTree: a tool for visual analysis of Caenorhabditis elegans embryogenesis. BMC Bioinformatics. 2006 Jun 1;7:275. PMCID: PMC1501046

63. Murray JI, Bao Z, Boyle TJ, Boeck ME, Mericle BL, Nicholas TJ, Zhao Z, Sandel MJ, Waterston RH. Automated analysis of embryonic gene expression with cellular resolution in C. elegans. Nat Methods. 2008 Jun;5(8):703–709.

Figure 1

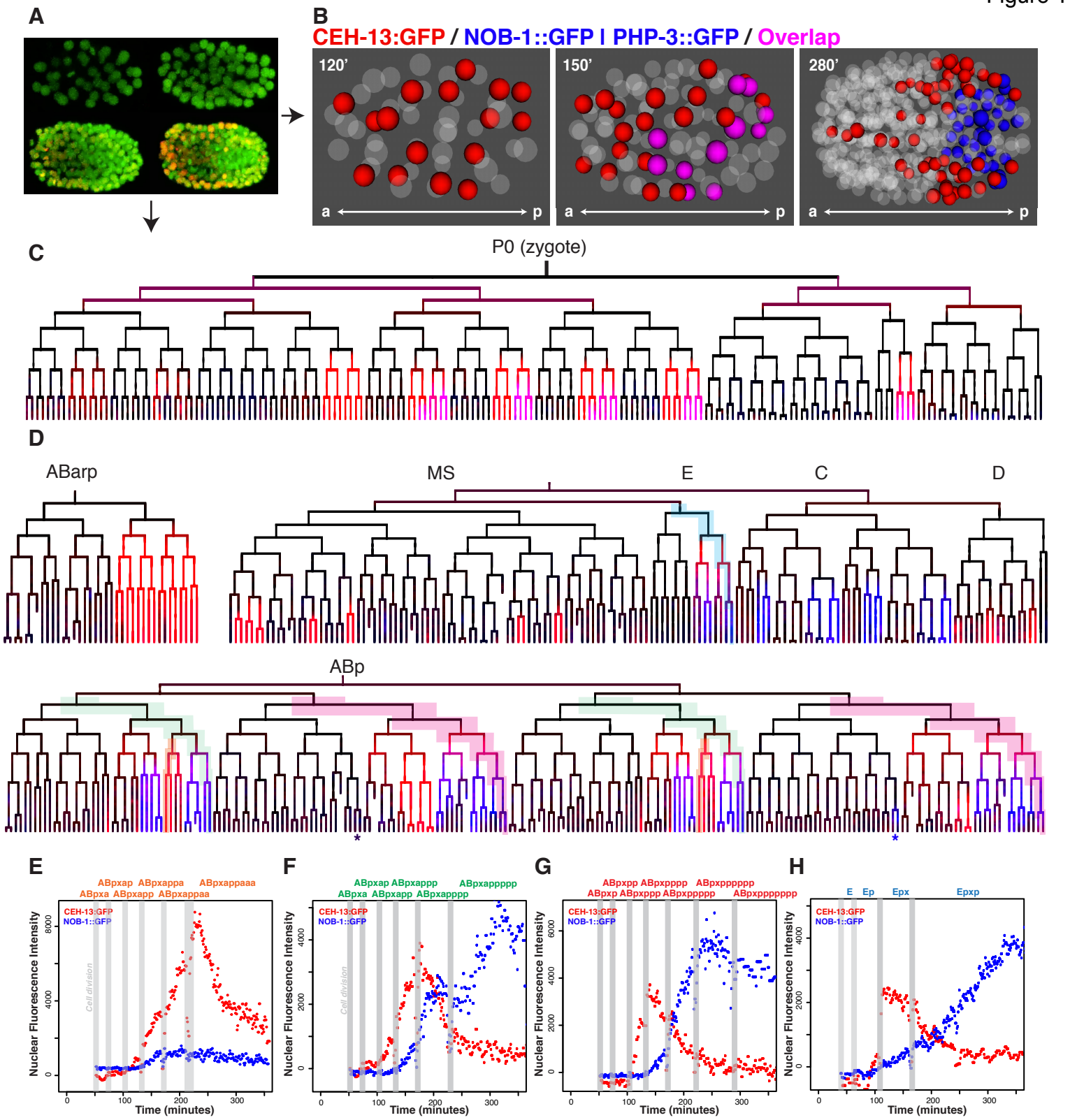
A
B
CEH-13:GFP / NOB-1::GFP I PHP-3::GFP / Overlap
120'
150'
280'
a
p
C
P0 (zygote)
D
ABarp
MS
E
C
D
ABp
E
ABpxap ABpxappa ABpxappaaa
ABpxa ABpxapp ABpxappaa
CEH-13:GFP
NOB-1::GFP
Cell division
Nuclear Fluorescence Intensity
Time (minutes)
F
ABpxap ABpxappp ABpxappppp
ABpxa ABpxapp ABpxappppp
G
ABpxpp ABpxpppp ABpxppppp
ABpxp ABpxppp ABpxpppp ABpxpppppp
H
E Ep Epx Epxp

Figure 2

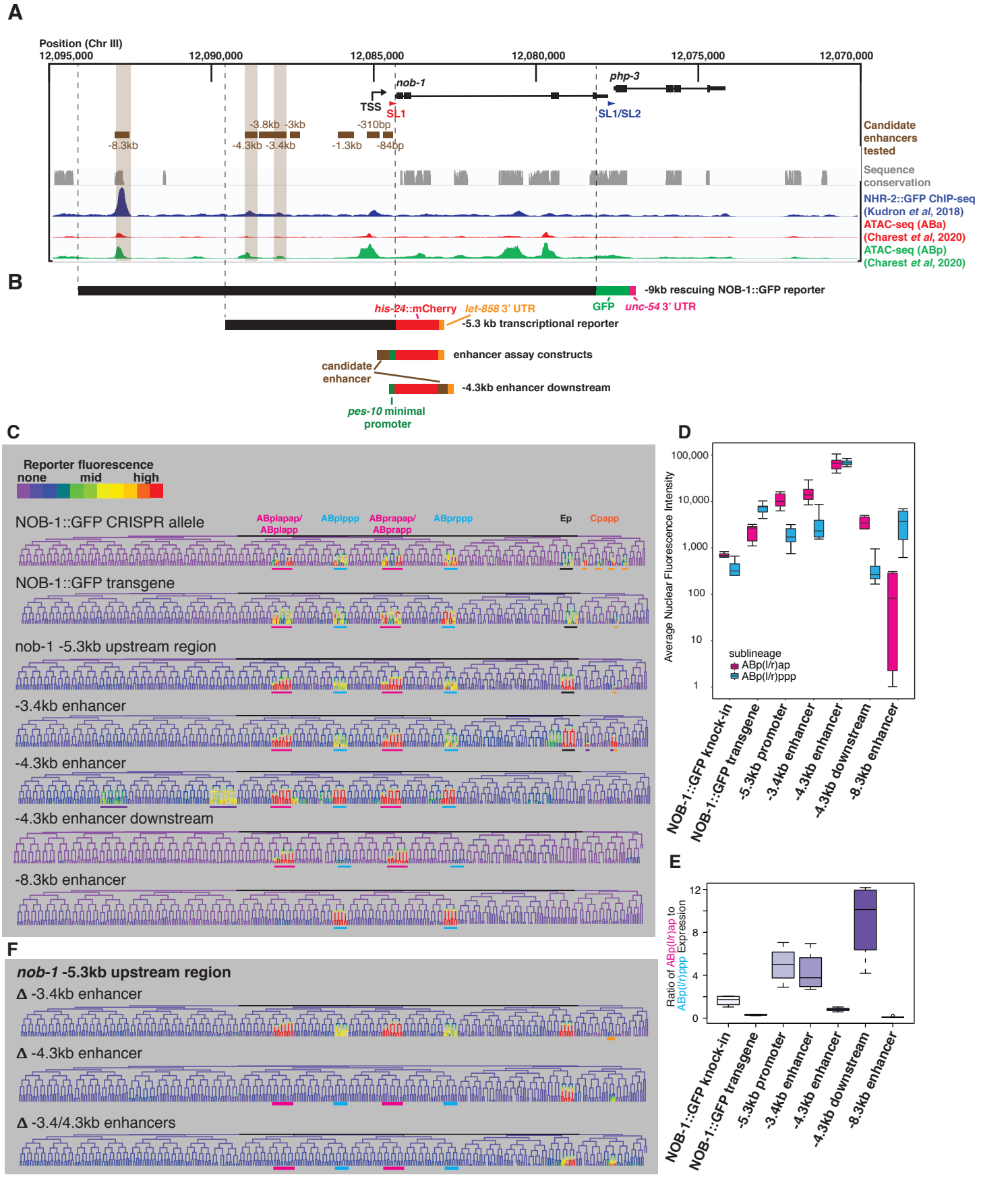
A
Position (Chr III)
12,095,000
12,090,000
12,085,000
12,080,000
12,075,000
12,070,000
nob-1
php-3
TSS
SL1
SL1/SL2
-8.3kb
-3.8kb
-3kb
-4.3kb
-3.4kb
-310bp
-1.3kb
-84bp
Candidate enhancers tested
Sequence conservation
NHR-2::GFP ChIP-seq (Kudron et al, 2018)
ATAC-seq (ABa) (Charest et al, 2020)
ATAC-seq (ABp) (Charest et al, 2020)
B
-9kb rescuing NOB-1::GFP reporter
his-24::mCherry
let-858 3' UTR
GFP
unc-54 3' UTR
-5.3 kb transcriptional reporter
enhancer assay constructs
candidate enhancer
-4.3kb enhancer downstream
pes-10 minimal promoter
C
Reporter fluorescence
none
mid
high
NOB-1::GFP CRISPR allele
ABplapap/ ABplapp
ABplppp
ABprapap/ ABprapp
ABprppp
Ep
Cpapp
NOB-1::GFP transgene
nob-1 -5.3kb upstream region
-3.4kb enhancer
-4.3kb enhancer
-4.3kb enhancer downstream
-8.3kb enhancer
D
Average Nuclear Fluorescence Intensity
100,000
10,000
1,000
100
10
1
sublineage
ABp(l/r)ap
ABp(l/r)ppp
NOB-1::GFP knock-in
NOB-1::GFP transgene
-5.3kb promoter
-3.4kb enhancer
-4.3kb enhancer
-4.3kb downstream
-8.3kb enhancer
E
Ratio of ABp(l/r)ap to ABp(l/r)ppp Expression
12
8
4
0
NOB-1::GFP knock-in
NOB-1::GFP transgene
-5.3kb promoter
-3.4kb enhancer
-4.3kb enhancer
-4.3kb downstream
-8.3kb enhancer
F
nob-1 -5.3kb upstream region
Δ -3.4kb enhancer
Δ -4.3kb enhancer
Δ -3.4/4.3kb enhancers

Figure 3

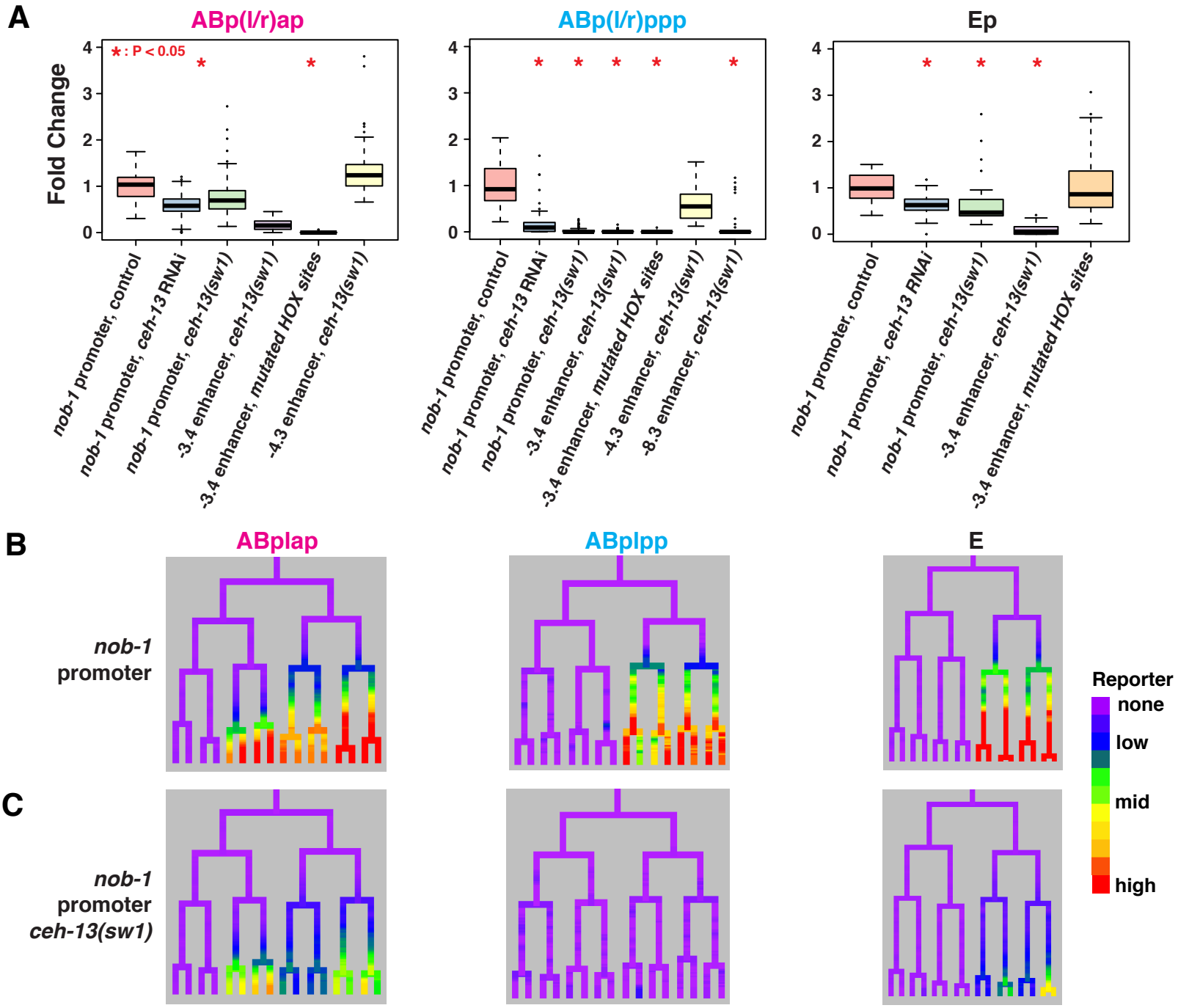
A
ABp(l/r)ap
ABp(l/r)ppp
Ep
Fold Change
* : P < 0.05
nob-1 promoter, control
nob-1 promoter, ceh-13 RNAi
nob-1 promoter, ceh-13(sw1)
-3.4 enhancer, ceh-13(sw1)
-3.4 enhancer, mutated HOX sites
-4.3 enhancer, ceh-13(sw1)
-8.3 enhancer, ceh-13(sw1)
B
ABplap
ABplpp
E
nob-1 promoter
C
nob-1 promoter ceh-13(sw1)
Reporter
none
low
mid
high

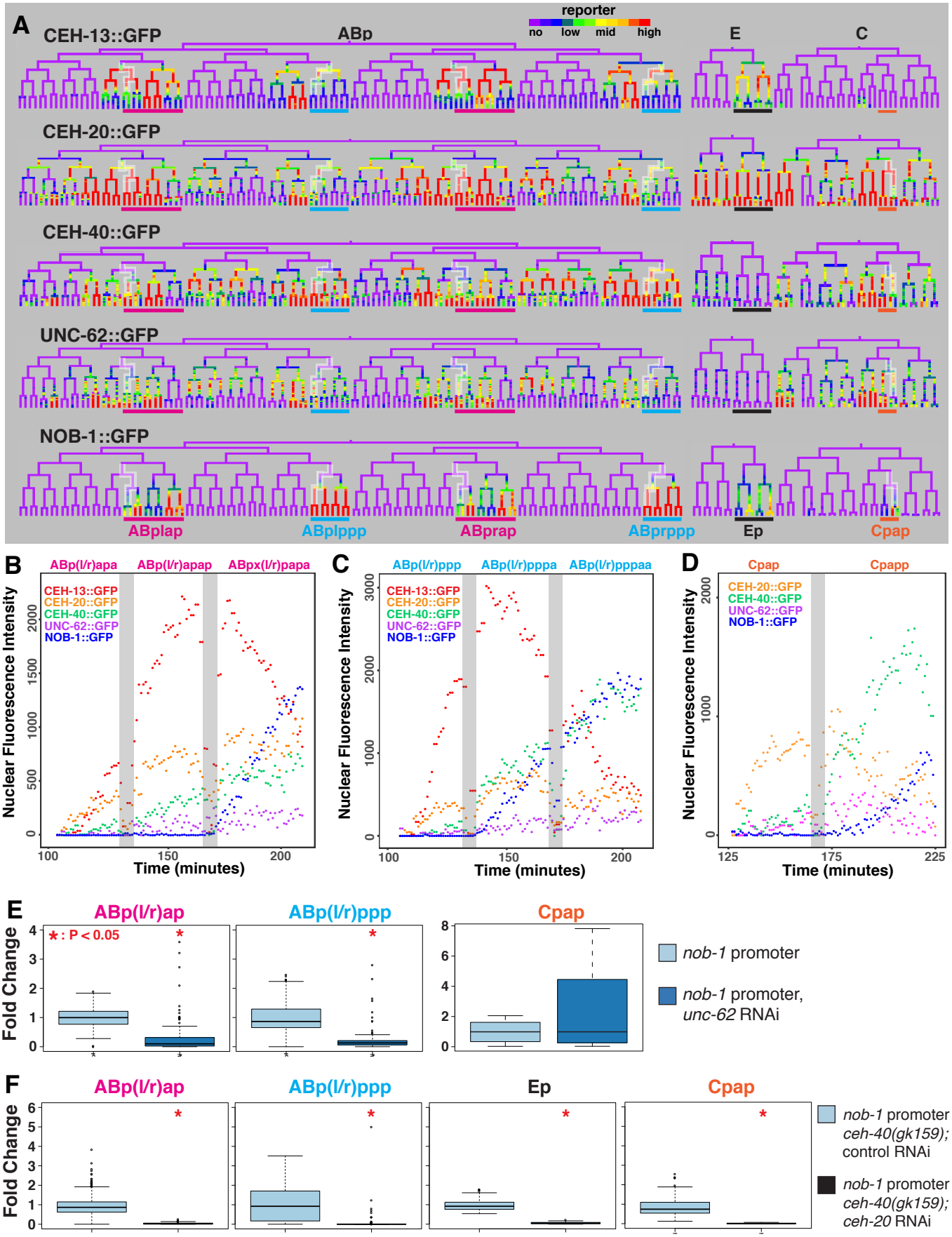
A
reporter
no
low
mid
high
CEH-13::GFP
ABp
E
C
CEH-20::GFP
CEH-40::GFP
UNC-62::GFP
NOB-1::GFP
ABplap
ABplppp
ABprap
ABprppp
Ep
Cpap
B
ABp(l/r)apa
ABp(l/r)apap
ABpx(l/r)papa
CEH-13::GFP
CEH-20::GFP
CEH-40::GFP
UNC-62::GFP
NOB-1::GFP
Nuclear Fluorescence Intensity
Time (minutes)
C
ABp(l/r)ppp
ABp(l/r)pppa
ABp(l/r)pppaa
D
Cpap
Cpapp
E
ABp(l/r)ap
ABp(l/r)ppp
Cpap
*: P < 0.05
Fold Change
nob-1 promoter
nob-1 promoter, unc-62 RNAi
F
ABp(l/r)ap
ABp(l/r)ppp
Ep
Cpap
nob-1 promoter ceh-40(gk159); control RNAi
nob-1 promoter ceh-40(gk159); ceh-20 RNAi

Figure 5

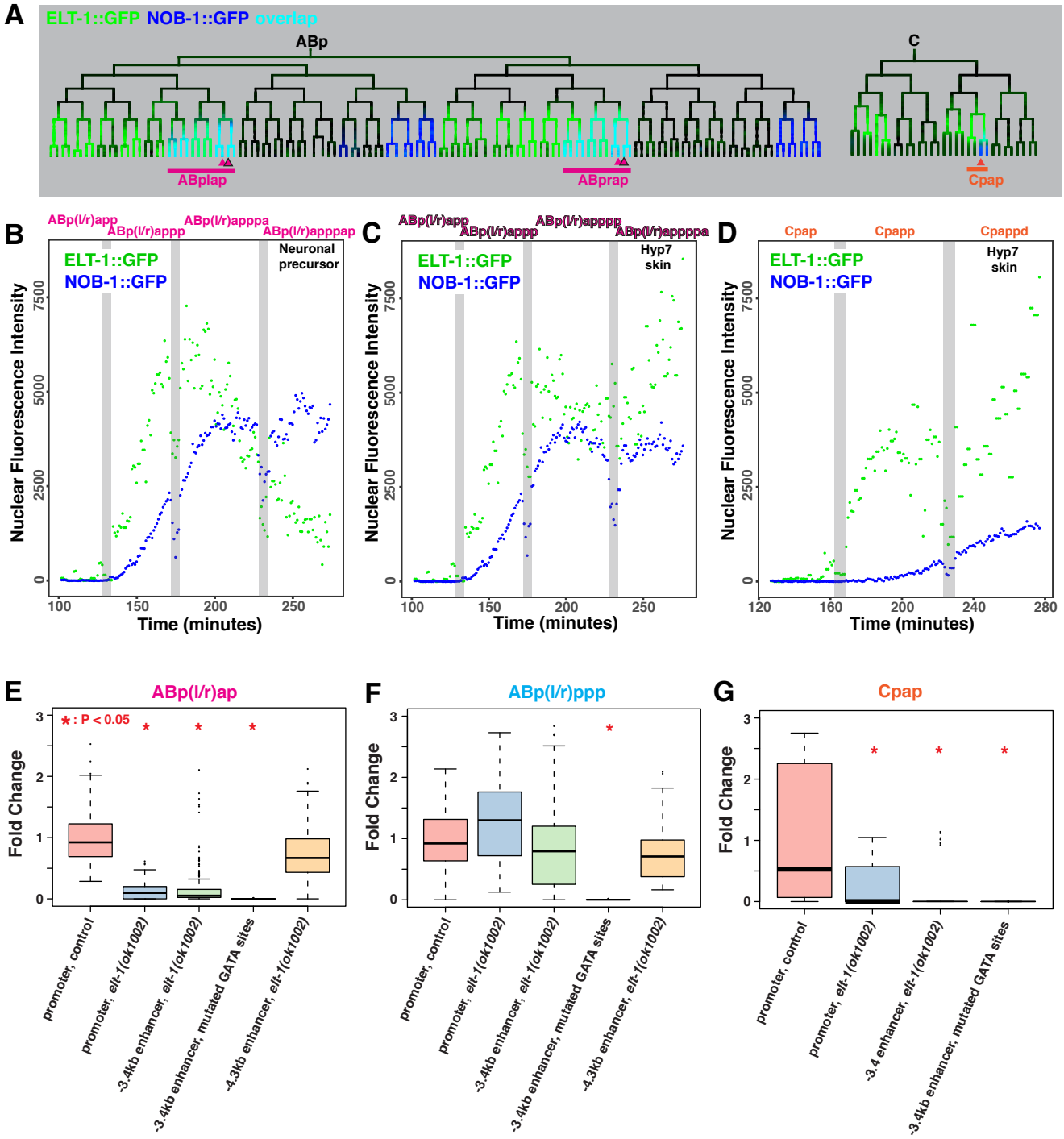
A
ELT-1::GFP NOB-1::GFP overlap
ABp
C
ABplap
ABprap
Cpap
B
ABp(l/r)app
ABp(l/r)appp
ABp(l/r)apppa
ABp(l/r)apppap
ELT-1::GFP
NOB-1::GFP
Neuronal precursor
Nuclear Fluorescence Intensity
Time (minutes)
C
ABp(l/r)app
ABp(l/r)appp
ABp(l/r)apppp
ABp(l/r)appppa
Hyp7 skin
D
Cpap
Cpapp
Cpappd
Hyp7 skin
E
ABp(l/r)ap
* : P < 0.05
Fold Change
promoter, control
promoter, elt-1(ok1002)
-3.4kb enhancer, elt-1(ok1002)
-3.4kb enhancer, mutated GATA sites
-4.3kb enhancer, elt-1(ok1002)
F
ABp(l/r)ppp
G
Cpap
-3.4 enhancer, elt-1(ok1002)

Figure 6

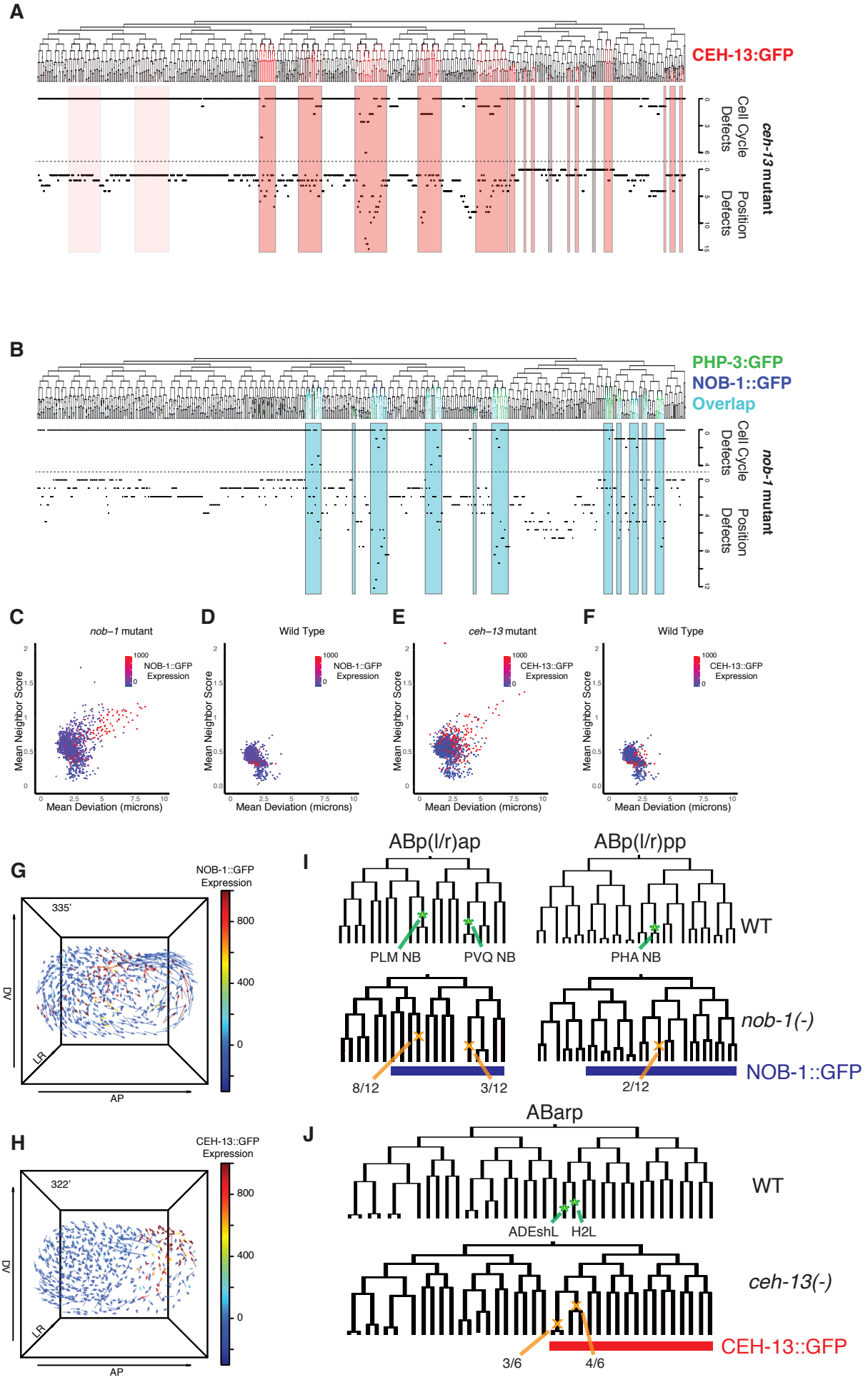
A
CEH-13:GFP
Cell Cycle Defects
Position Defects
ceh-13 mutant
B
PHP-3:GFP
NOB-1::GFP
Overlap
Cell Cycle Defects
Position Defects
nob-1 mutant
C
nob−1 mutant
NOB-1::GFP Expression
Mean Neighbor Score
Mean Deviation (microns)
D
Wild Type
NOB-1::GFP Expression
E
ceh−13 mutant
CEH-13::GFP Expression
F
Wild Type
CEH-13::GFP Expression
G
NOB-1::GFP Expression
335'
DV
LR
AP
H
CEH-13::GFP Expression
322'
I
ABp(l/r)ap
ABp(l/r)pp
WT
PLM NB
PVQ NB
PHA NB
nob-1(-)
8/12
3/12
2/12
NOB-1::GFP
J
ABarp
WT
ADEshL
H2L
ceh-13(-)
3/6
4/6
CEH-13::GFP

Figure S1

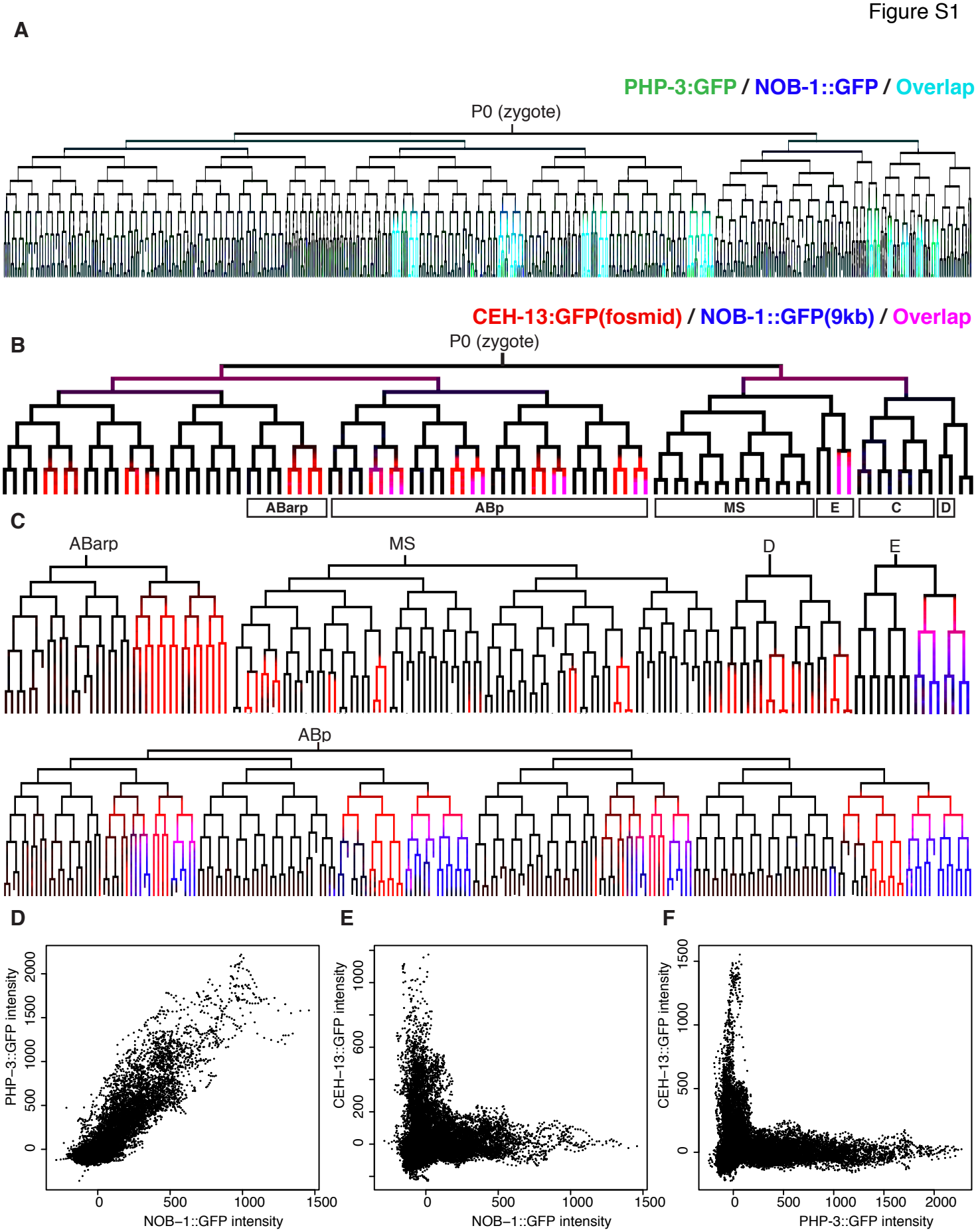
A
PHP-3:GFP / NOB-1::GFP / Overlap
P0 (zygote)
B
CEH-13:GFP(fosmid) / NOB-1::GFP(9kb) / Overlap
P0 (zygote)
ABarp
ABp
MS
E
C
D
C
ABarp
MS
D
E
ABp
D
PHP−3::GFP intensity
NOB−1::GFP intensity
E
CEH−13::GFP intensity
NOB−1::GFP intensity
F
CEH−13::GFP intensity
PHP-3::GFP intensity

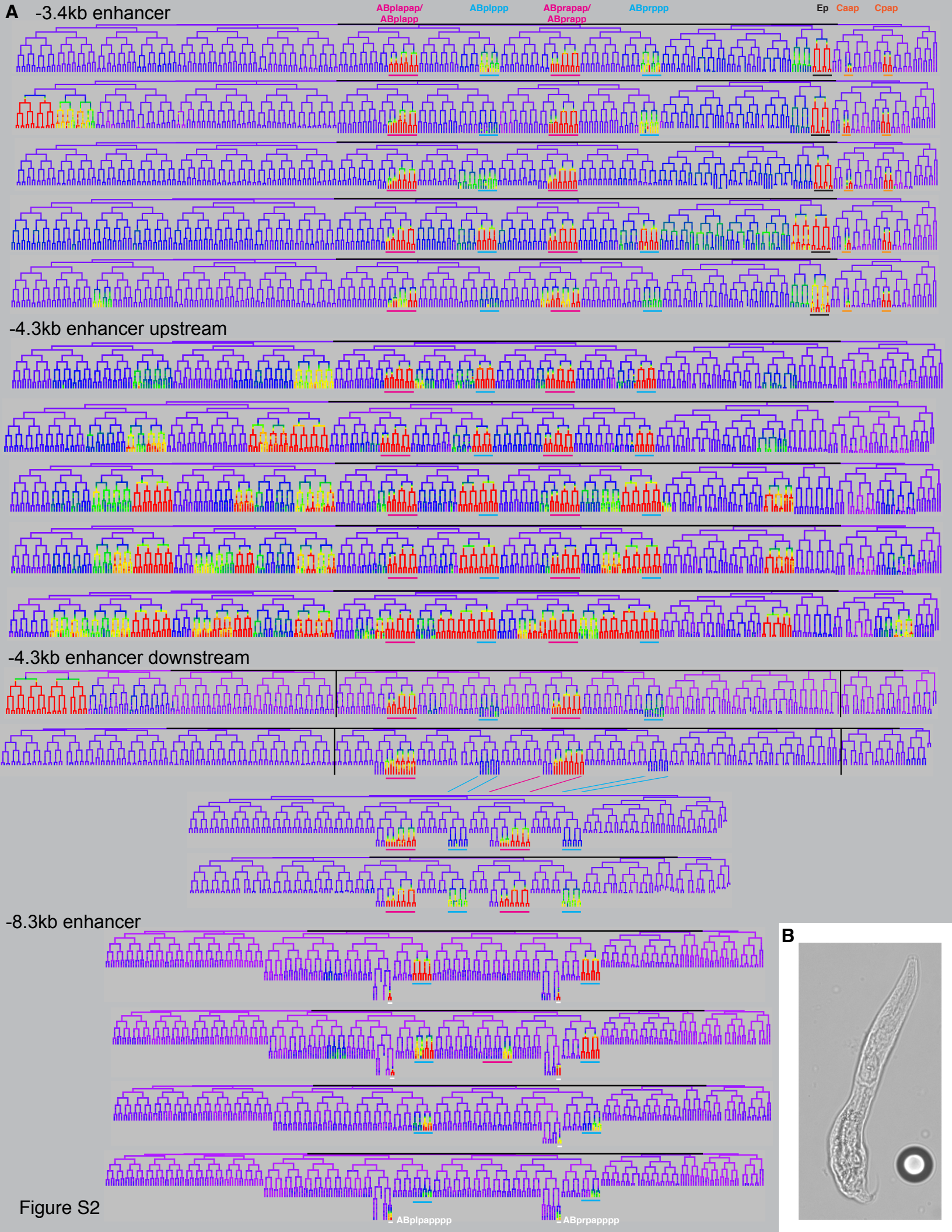
A
-3.4kb enhancer
ABplapap/
ABplapp
ABplppp
ABprapap/
ABprapp
ABprppp
Ep
Caap
Cpap
-4.3kb enhancer upstream
-4.3kb enhancer downstream
-8.3kb enhancer
ABplpapppp
ABprpapppp
B

Figure S2

Figure S3

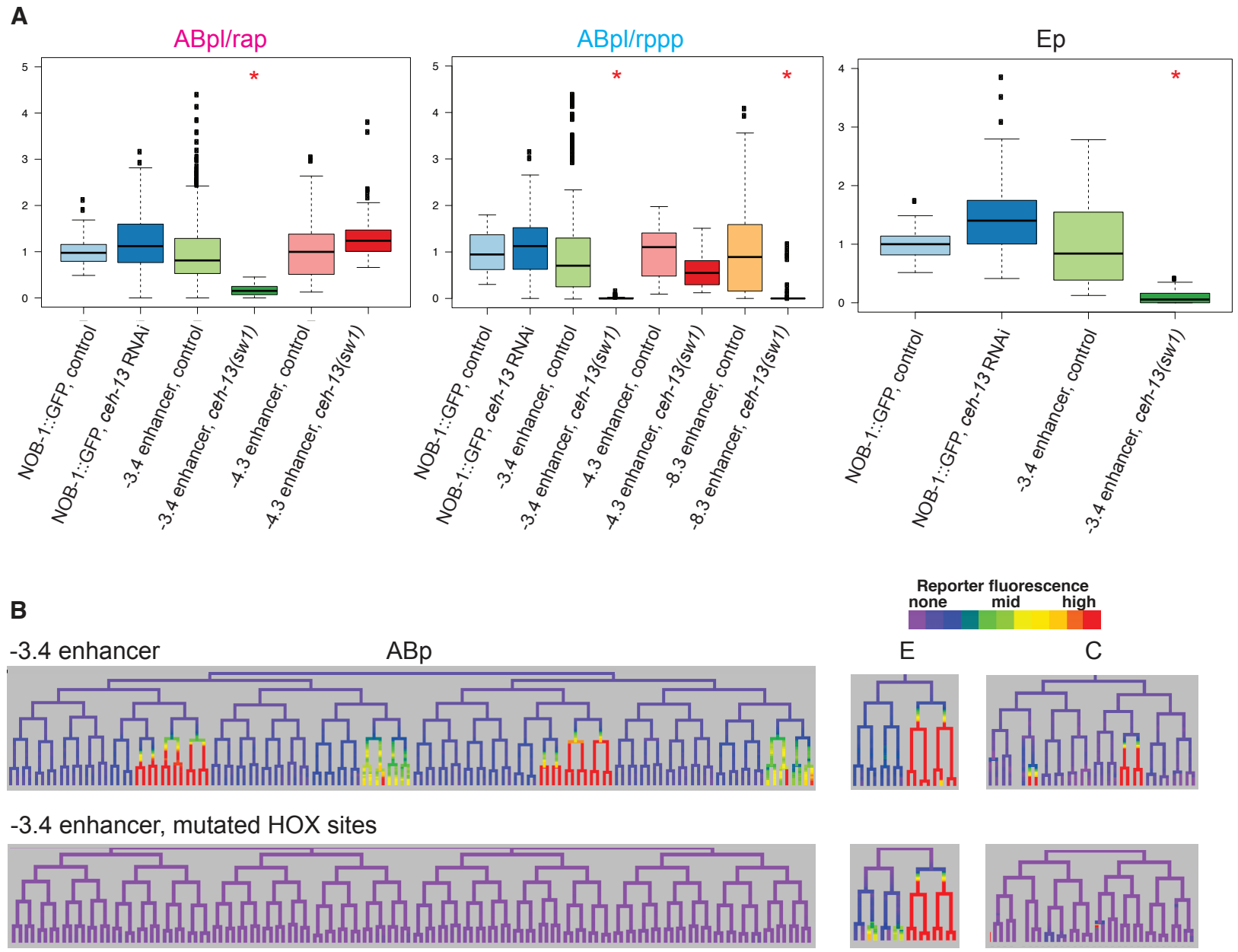
A
ABpl/rap
ABpl/rppp
Ep
*
NOB-1::GFP, control
NOB-1::GFP, ceh-13 RNAi
-3.4 enhancer, control
-3.4 enhancer, ceh-13(sw1)
-4.3 enhancer, control
-4.3 enhancer, ceh-13(sw1)
-8.3 enhancer, control
-8.3 enhancer, ceh-13(sw1)
B
Reporter fluorescence
none
mid
high
-3.4 enhancer
ABp
E
C
-3.4 enhancer, mutated HOX sites

Figure S4

A *nob-1* promoter, ABpl sublineage

control

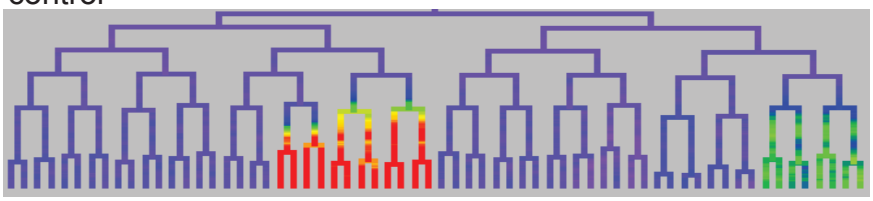

unc-62 RNAi

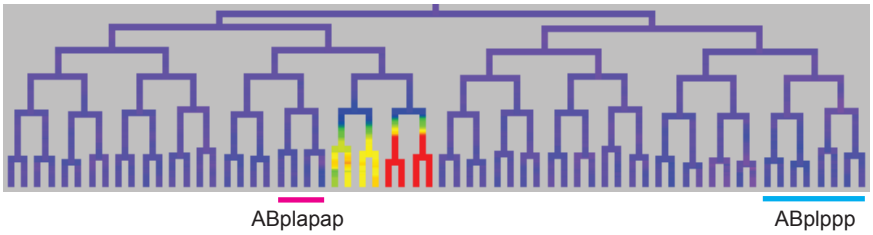

B NOB-1::GFP, ABpr sublineage

control

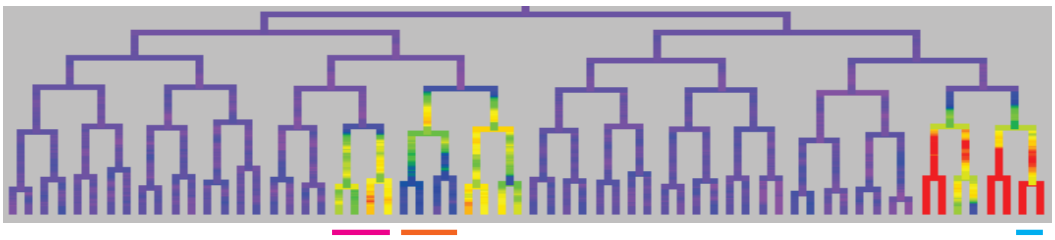

unc-62 RNAi

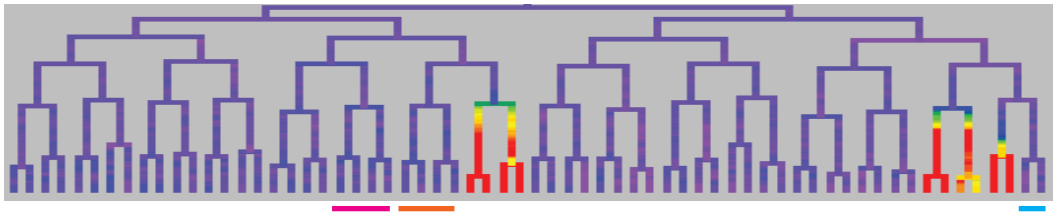

example #1

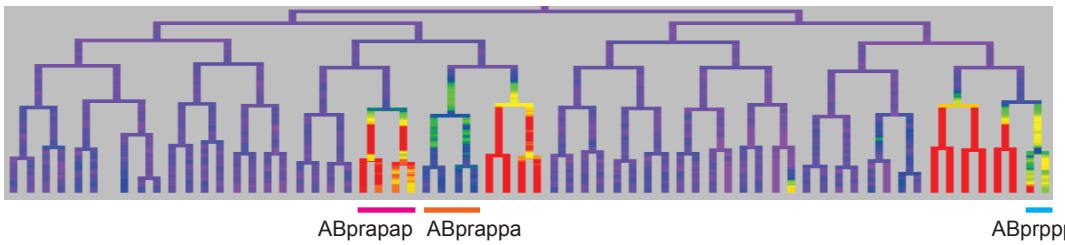

example #2

C

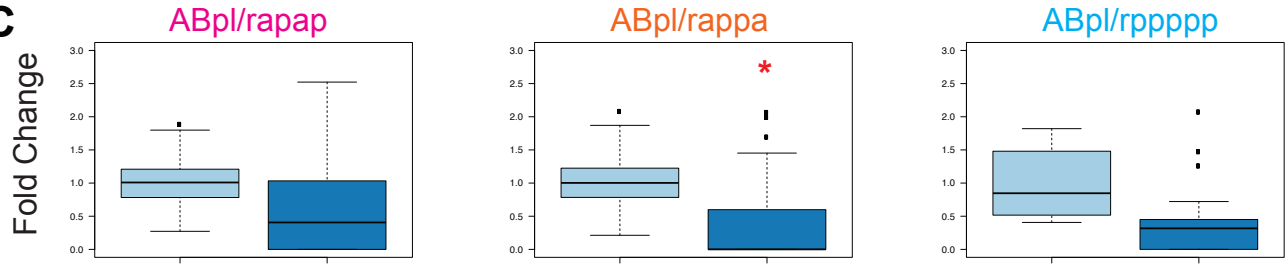

D

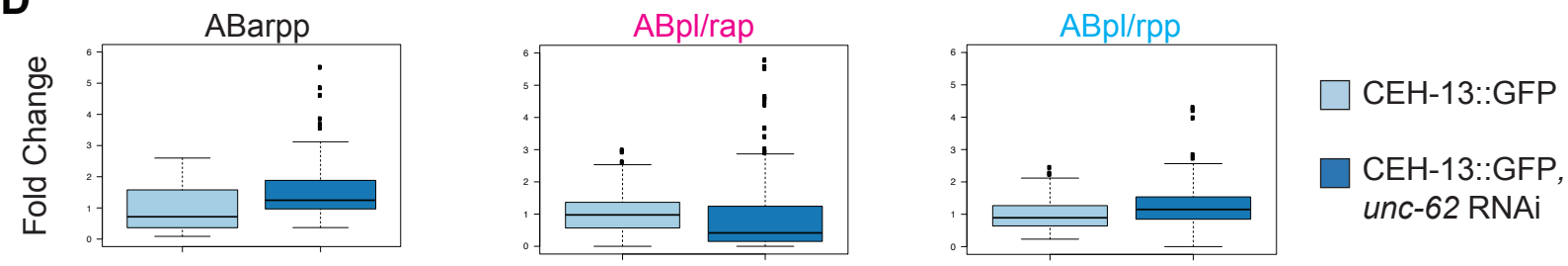

Figure S5

CEH-20::GFP

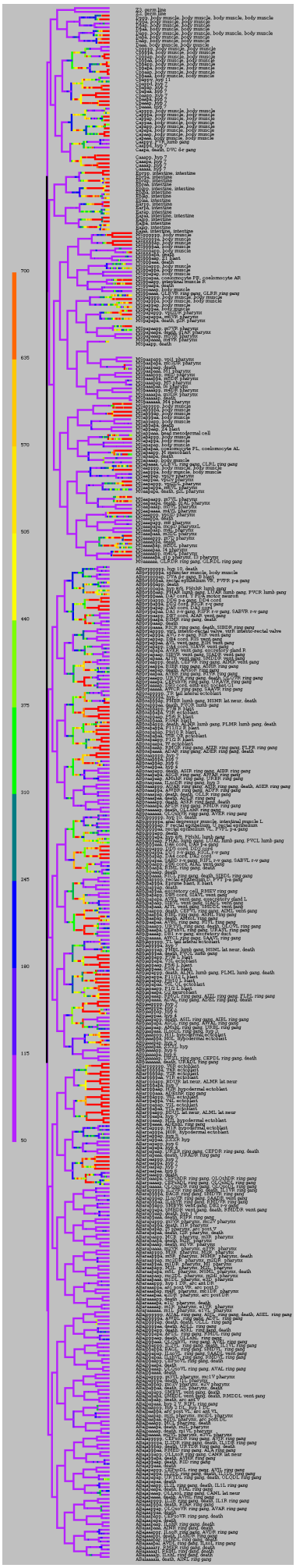

CEH-40::GFP

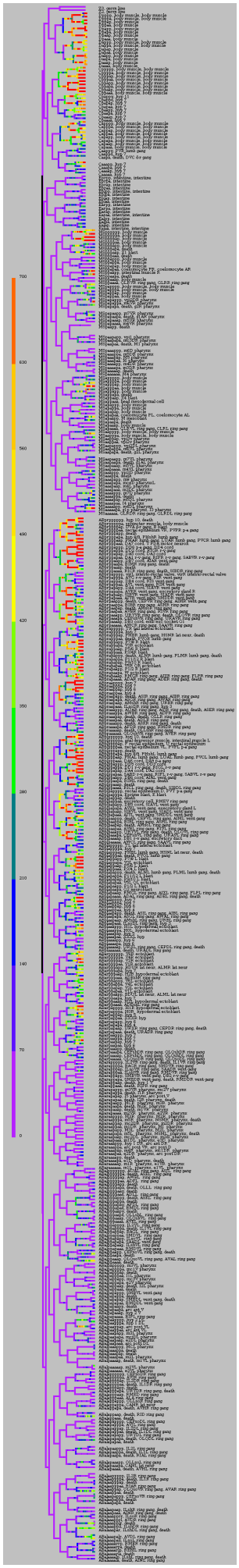

UNC-62::GFP

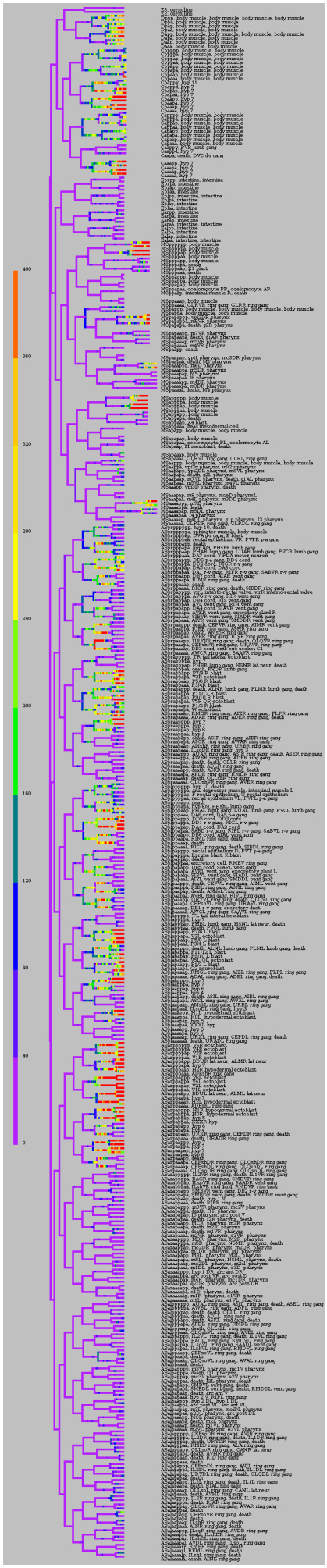

ELT-1::GFP

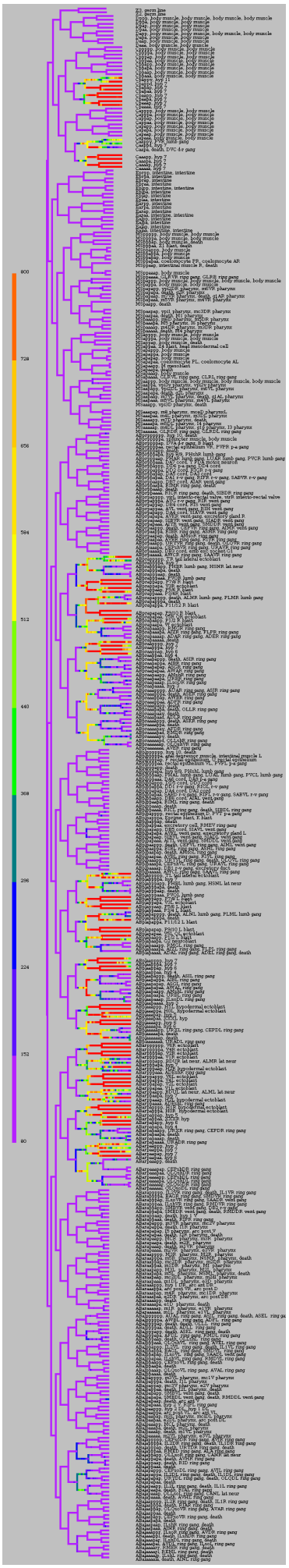

Figure S6

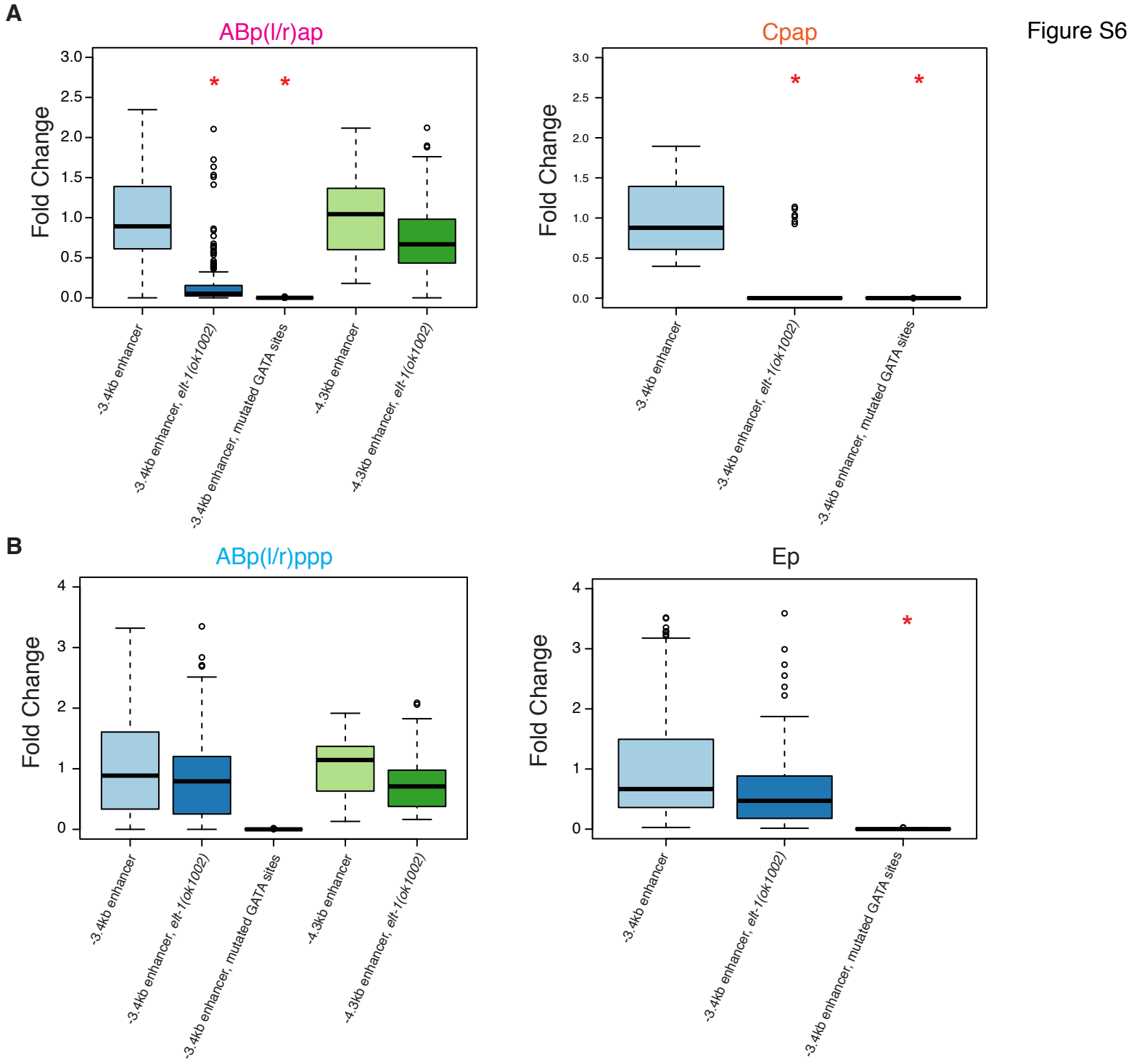
A
ABp(l/r)ap
Cpap
Fold Change
-3.4kb enhancer
-3.4kb enhancer, elt-1(ok1002)
-3.4kb enhancer, mutated GATA sites
-4.3kb enhancer
-4.3kb enhancer, elt-1(ok1002)
B
ABp(l/r)ppp
Ep
C
Reporter fluorescence
none
mid
high
-3.4kb enhancer
ABp
E
C
-3.4kb enhancer, mutated GATA sites

Figure S7

A

ABp

Wildtype

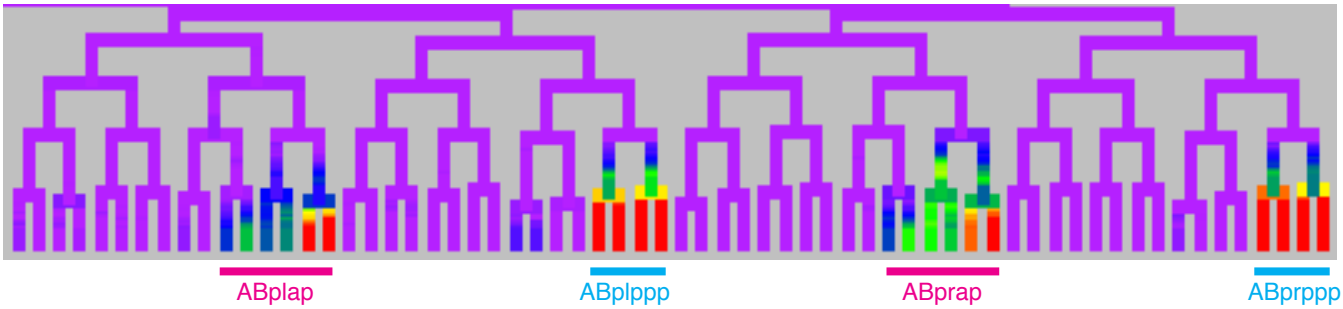

unc-30(ok613); ceh-36(ok795)

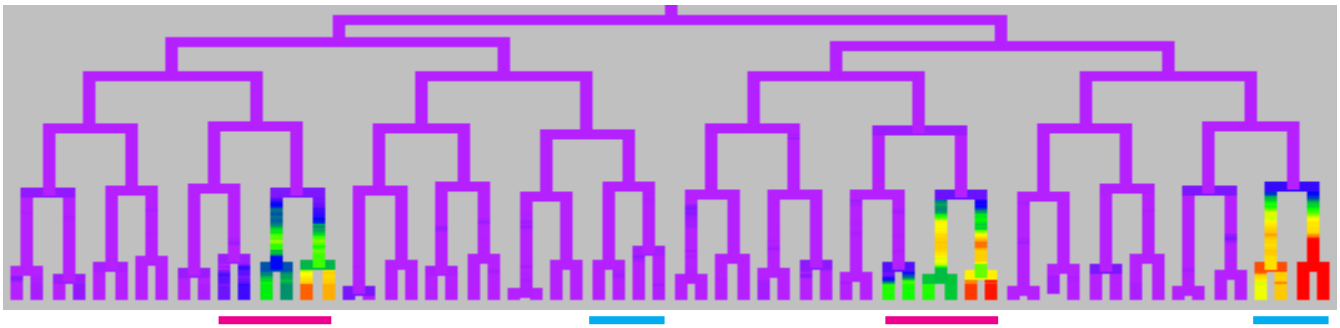

unc-30(ok613); ceh-36(ok795)

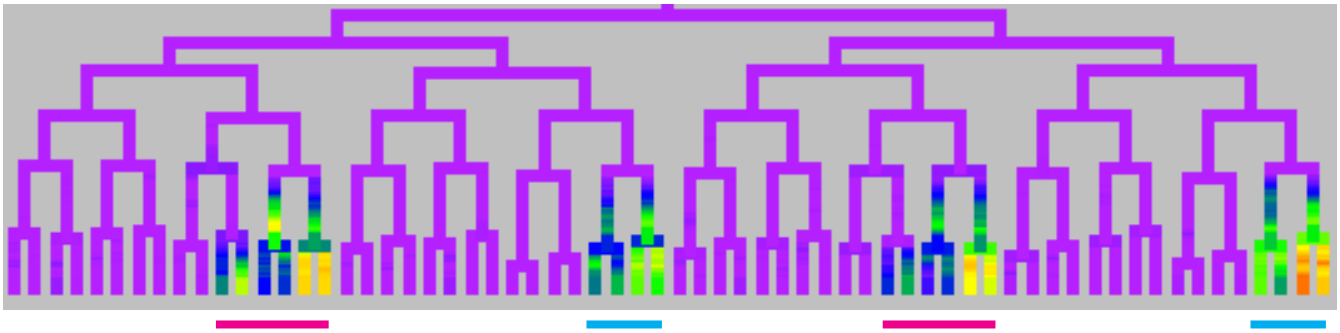

B

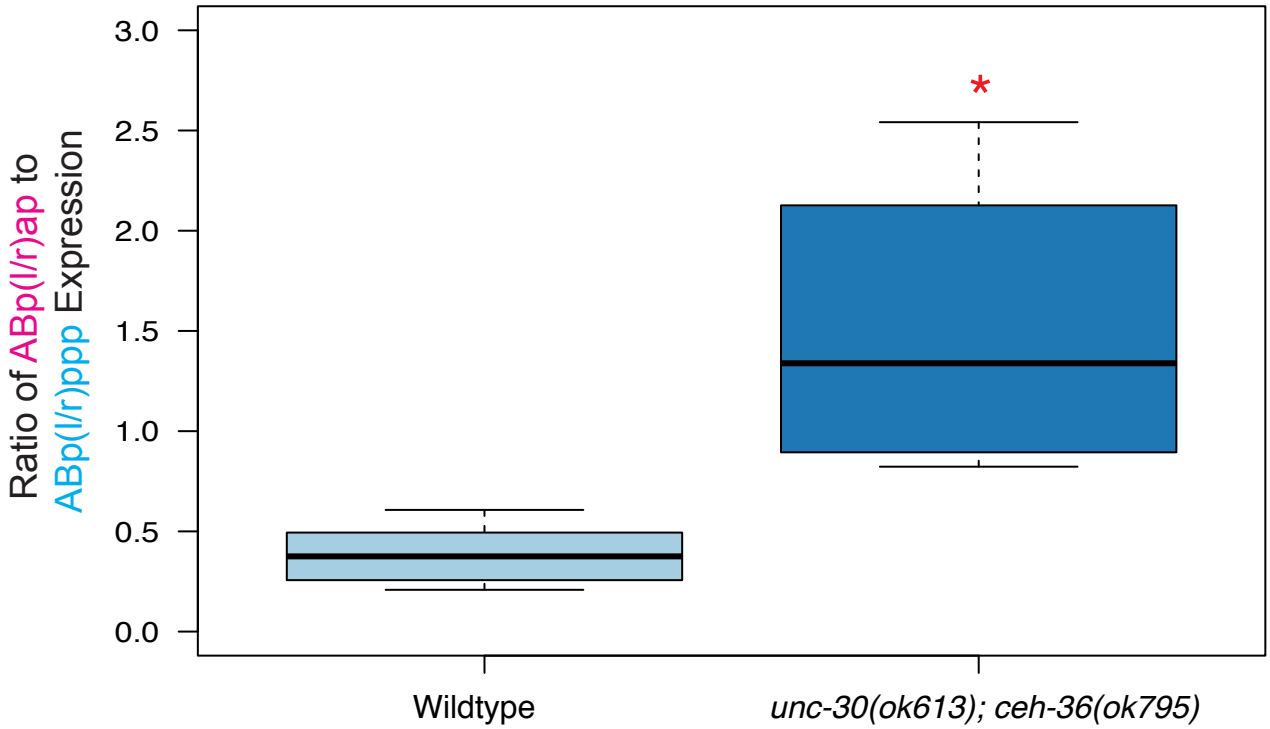

Figure S8

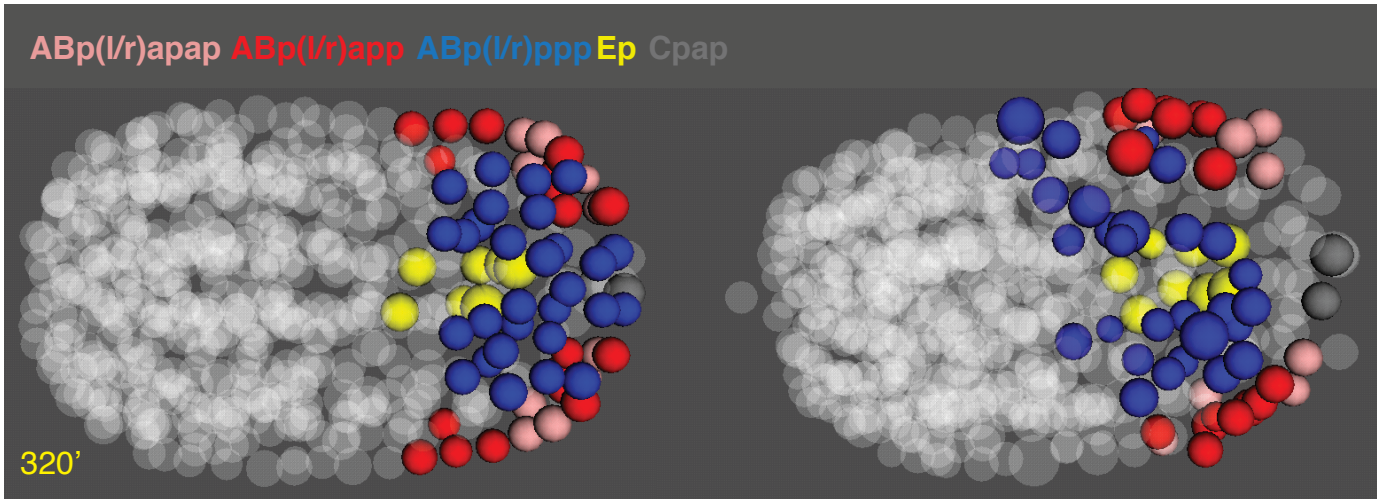

Wild Type ***nob-1(ct223)***

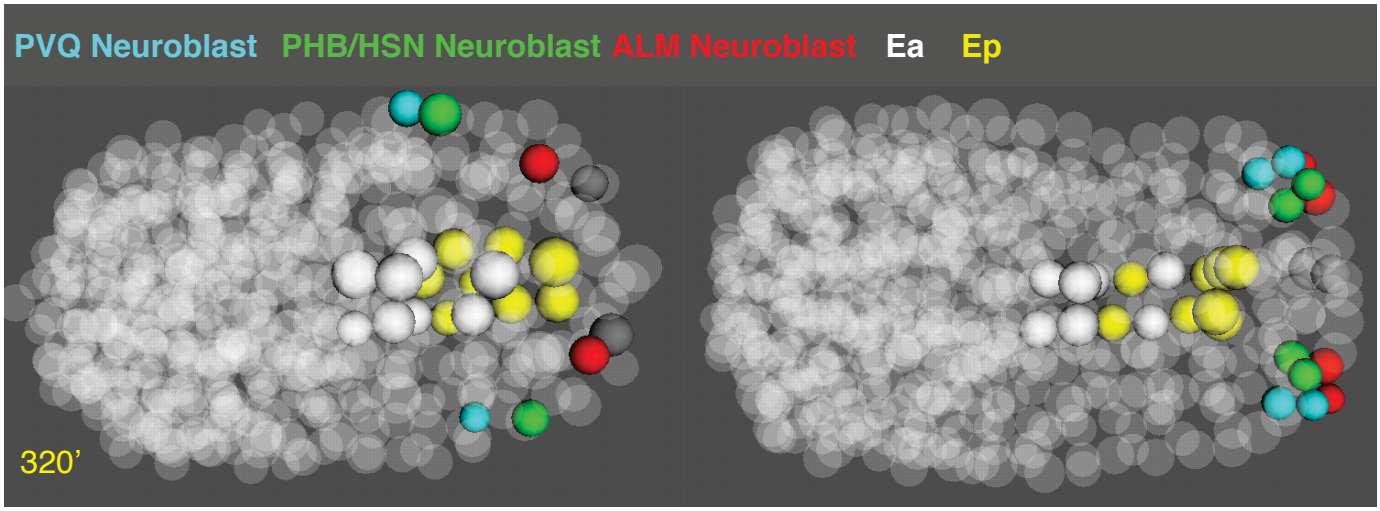

Wild Type ***nob-1(ct223)***